A systematic comparison of cooperation and coordination across behavioural, psychological, and neural scales

Yang Li[1,3], Xin Wang[1,2,3,4,5*], Wucheng Dong[1,3], Longzhao Liu[1,2,3,4,5], Yaqian Yang[1,3], Yi Zheng[1,3,4], Yi Zhen[2,3], Hongwei Zheng[9], Shaoting Tang[1,2,3,4,5,6,8*]

[1]School of Artificial Intelligence, Beihang University, Beijing 100191, China.
[2]Hangzhou International Innovation Institute, Beihang University, Hangzhou 311115, China.
[3]Key laboratory of Mathematics, Informatics and behavioural Semantics, Beihang University, Beijing 100191, China.
[4]Beijing Advanced Innovation Center for Future Blockchain and Privacy Computing, Beihang University, Beijing 100191, China.
[5]Zhongguancun Laboratory, Beijing 100094, China.
[6]State Key Laboratory of Complex & Critical Software Environment, Beihang University, Beijing 100191, China.
[7]Institute of Trustworthy Artificial Intelligence, Zhejiang Normal University, Hangzhou 310012, China.
[8]Institute of Medical Artificial Intelligence, Binzhou Medical University, Yantai 264003, China.
[9]Beijing Academy of Blockchain and Edge Computing, Beijing 100085, China.

*Corresponding author(s). E-mail(s): wangxin_1993@buaa.edu.cn; tangshaoting@buaa.edu.cn;

Abstract

Cooperation and coordination are the two fundamental mechanisms for enhancing social welfare. However, the intrinsic differences between the dynamics of cooperation and coordination remain elusive, particularly from an interpretable perspective that bridges behavioural, psychological, and neural scales. Here, we compare and analyze cooperation and coordination within a unified framework by assigning participants to an adjustable public goods game for iterated real-time interactions. By integrating model-free behavioural patterns and psychological intentions, we show that individuals are driven by increased flexibility and are more susceptible to peer influence in decision-making under cooperation. While under coordination, it is easier to reach the group consensus, inspiring individuals to stick more closely to their existing behavioural patterns and the 'default' social norms. Furthermore, although peer punishment can enhance reciprocal contributions in all scenarios, the detailed impact and the resultant adverse phenomena (anti-social punishment) in cooperation and coordination are different. Notably, behavioural motive differences are also reflected in the neural responses recorded via fNIRS, in which coordination is associated with activation of the rTPJ and more consistent inter-brain synchronization in the dmPFC, while there is a negative correlation between dmPFC–rTPJ connectivity and contributions under cooperation. In addition, rTPJ during the punishment phase is significantly activated compared with the investment phase. Our study systematically reveals the fundamental differences between cooperation and coordination at the multi-scale levels, which not only deepens the understanding of reciprocal behaviour in social groups, but also provides a foundation for designing targeted incentive mechanisms.

Introduction

In today's highly interconnected and diverse world, people face complex interactive decision-making processes [1–3]. These interactions shape not only the destinies of individuals but also the trajectories of collectives [4], as evidenced in areas such as corporate alliances, environmental protection, and disease control. Enhancing social welfare is a fundamental objective of such social interactions. Unfortunately, the singular pursuit of individual interests frequently results in the damage of collective interests, consequently diminishing social welfare and giving rise to a social dilemma [5, 6]. For instance, over-exploitation of common resources by individuals may lead to resource depletion. Similarly, inaction by certain countries in climate change mitigation efforts can impede the achievement of global environmental goals. Iterated games, which give rise to direct reciprocity [7, 8], are considered an effective mechanism to overcome the dilemma. Individuals anticipate future benefits from their current behaviour and are thus willing to forgo short-term personal gains in exchange for long-term collective benefits. Consequently, understanding and predicting collective behaviour in frequent interactions has become a crucial issue [9, 10].

Recent research, aiming at the basic issues of social orders and norms, has begun to differentiate between the broad types of reciprocal behaviour that can enhance social welfare [11, 12]. This has given rise to two fundamental social mechanisms: cooperation and coordination [13–15]. Although the prisoner's dilemma and battle of the sexes can represent the two mechanisms in a dyadic context [12], many of the most pressing problems has taken the form of large-scale social dilemmas in the world with numerous participants. The public goods game (PGG), which is a variant of group behaviour game that evolves from the expansion of simple pairwise interactions, can be a natural tool for studying multi-person interactive decision-making [16, 17], leading to the development of linear and nonlinear PGGs (including the volunteer's dilemma [18]). Under the cooperation mechanism, after the public pool expands, the individuals' contributions forms a reward and then distributed among all group members without any loss. Under the coordination mechanism, a threshold is established for the public pool. If the contributions fail to meet it, no reward is generated; otherwise, a reward equal to the threshold is evenly distributed. For instance, Joseph Pulitzer initiated a crowdfunding campaign through the New York World to raise funds for constructing the pedestal of the Statue of Liberty in the 19th century [19]. From a Nash-equilibrium perspective, cooperation has a unique equilibrium characterised by a complete absence of contributions, while coordination additionally has a partial contribution Nash equilibrium (Pareto optimal solution).

Currently, the dynamics of cooperation and coordination have been extensively studied. Evolutionary game theory assumes bounded rationality and investigates how individuals with learning capabilities can adaptively develop cooperation and coordination among populations [18, 20]. Previous studies have examined the impact of endowment and productivity heterogeneity on relative contributions, revealing that overall welfare is maximized when these two sources of heterogeneity are aligned in cooperation [21]. Subsequent research has further quantified the degree of this inequality and found that the optimal endowment allocation is located on the Pareto frontier between resilience and efficiency [22]. While in coordination, individuals may strive to equalize their relative contributions in relation to their endowments and contribute equally even when productivity varies [23]. Furthermore, cooperation and coordination behaviours differ significantly in the context of optional public goods. Specifically, optional public goods tend to increase contributions in coordination [24], whereas they often favor anti-social punishment in cooperation [25].

Moreover, the intentions of humans to modify their behavioural strategies can be mirrored in the neural basis [26]. It has been proved that mutually cooperative social interactions are associated with activation in anteroventral striatum, rostral anterior cingulate cortex (ACC), and orbitofrontal cortex

(OFC) in the prisoner's dilemma game of cooperative mechanisms [27], while in the binary selection coordination of the volunteer's dilemma, the prefrontal cortex (PFC) computes the selection utility, which is tracked and updated by the temporoparietal junction (TPJ) and the anterior cingulate gyrus (ACCg) [28]. In fact, a large body of research has investigated the human capacity to mentalize about others and to dynamically update beliefs that predict others' behaviour, including simple selection prediction [29–31], dyadic reciprocity and competition [32, 33], and the spread of opinion in social networks [34]. They found that certain brain regions such as the medial prefrontal cortex (dmPFC/vmPFC), TPJ, dorsal anterior cingulate cortex (dACC), and posterior superior temporal sulcus (pSTS) play a crucial role in human prediction abilities and laid a solid foundation for research related to cognition. Additionally, there have been reviews clarifying that norm enforcement is also enabled through repurposing of basic cognitive mechanisms [35]. So far, studies have compellingly illustrated the significant roles of the mPFC and the TPJ to the formation of group consensus [36] and the enforcement of third-party punishment [37].

Despite the process, the underlying behavioural motives that drive and differentiate group cooperation and coordination remain largely unknown, calling for a comprehensive and interpretable framework that integrates behavioural, psychological, and neural scales to elucidate the specific characteristics of group reciprocity under cooperation and coordination. What constitutes the fundamental distinction between the mechanisms of cooperation and coordination in real world behaviour? Intuitively, when individuals repeatedly make restrictive selections in PGGs, the two mechanisms may elicit disparate psychological states, thereby leading to different behavioural strategies and neural patterns. Even though there is a single Nash equilibrium in cooperation, direct reciprocity can lead to deviations from zero-contribution decisions. Due to the lack of a unified contribution standard, behaviour might be more flexible in groups [38]. Conversely, the threshold unique to the coordination mechanism offers a clearer decision-making goal [39, 40]. Motivated by the goal value, individuals can facilitated a more consistent consensus within the group [41].

Here, we propose a multidimensional framework for comparing cooperation and coordination. Specifically, we integrated the findings from psychological intentions and neural feedback in a real behaviour experiment based on a real-time interactive paradigm of the iterated public goods game [42], and systematically elucidated the fundamental differences between cooperation and coordination across various scales. These manipulations in a laboratory setting [43] simulate the nature of real-world social interactions generating welfare in two aspects. Participants' productivity reflecting the level of skill was strategically regulated, which mimicked individual capability heterogeneity. The implementation of second-order public goods was then achieved through allowing peer punishment [44, 45]. Participants could sacrifice their own fixed wealth to impose a substantial fine on designated individuals in rounds with punishment phase. Neurally, we used functional near-infrared spectroscopy (fNIRS) hyperscanning [46–49], a neuroimaging method that can record brain hemodynamics in multiple subjects simultaneously, to allow analysis of neural responses with minimal disruption to group decision-making [50]. The PFC (especially the dmPFC) and rTPJ are together considered to support the unique social intention of human beings [51–53]. The rTPJ is involved in processing actions and cues related to social contexts, inferring social intentions, and engaging in psychological theory of mind. Meanwhile, the dmPFC may regulate the automatic sharing of representations among social partners and contribute to social learning [54]. So, we set these two regions as regions of interest for measurement.

We establish a psychological computational framework that can encompass cooperation and coordination behaviour using the utility strategy model [55, 56] (For detailed insights, refer to the recent study [57]). We firstly highlight differences in behavioural representation of the two mechanisms

within this framework. The SON (Self-regarding, Others, and Norms) utility strategy model [55, 56], based on beliefs about others' decisions [28], effectively explains the experimental behavioural data. Comparatively, cooperation drives flexibility while coordination promotes consensus. In particular, participants' decisions were highly flexible and easily influenced by others through the higher imitation coefficients under cooperation. In contrast, participants exhibited a tendency to stick to past decisions and adhere to the consensus through the higher stickiness coefficients and absolute values of social norms parameters in the SON model under coordination. We also found that peer punishment can promote social norm enforcement, while the impacts of various dimensions, especially the increase of contributions and the type of punishments, are different between cooperation and coordination [41, 58]. In the round dimension, the mean contributions of participants with varying productivity exist differences, which are distinct when compared under conditions of cooperation and coordination. Neural-scale results are in line with behavioural results. Specifically, both neural activation and inter-brain neural synchronization (INS) are markedly higher under coordination than under cooperation, consistent with individuals' stricter adherence to social norms under coordination. Furthermore, we found that the overall decision's linear correlation with neural responses varied across different mechanisms. Activation is positively correlated with contributions while INS is negatively correlated with behavioural similarity under coordination. In addition, dmPFC–rTPJ connectivity is negatively correlated with contributions under cooperation.

Results

We employed a 2×2 mixed factorial design: between-subjects factor (cooperation vs. coordination) and within-subjects factor ([peer] punishment vs. no [peer] punishment). A total of 540 participants were randomly assigned to 135 four-person groups and completed a real-time interactive task. During the experiment, all participants wore multi-channel fNIRS headsets to record hemodynamics from predefined brain regions of interest. The task was a iterated PGG consisting of three phases per round: investment, punishment (P rounds), and outcome display (Figure 1a). Each participant received an endowment of 30 points at the beginning of each round and simultaneously selected one of seven possible contributions on the slider (0, 5, 10, 15, 20, 25, or 30 points). Points contributed by participants (i.e., contributions) were multiplied by a productivity (low productivity [=1.6] or high productivity [=3.2]) and added to a corporate wealth. The corporate wealth was divided equally among all four members under cooperation, while the corporate wealth was compared with a pre-set threshold under coordination. If the wealth met or exceeded the threshold, each member received a share equivalent to a quarter of the threshold; otherwise, no wealth was distributed. Each group completed 51 rounds divided into four stages: preparation stage (rounds 1–6), first no punishment stage (NP1, rounds 7–21), punishment stage (P, rounds 22–36), and second no punishment stage (NP2, rounds 37–51). During the punishment stage, participants could assign punishment points (i.e., punishments) at a cost of 2 points to reduce the wealth of any other group member by 6 points. The entire experimental procedure was conducted on the day of the main experiment and lasted approximately 100 minutes. This duration encompassed the delivery of instructions, comprehension checks, the main task, and the post-experiment survey. (see Method Main experiment for full details).

Model-free behaviour patterns of cooperation-coordination

To capture the heterogeneity in real-world group productivity [21, 23, 59, 60], we manipulated the number of high-productivity participants ($p = 3.2$) across treatments ($n_{HPP} = 1, 2$). We firstly

showed the mean contributions of high-productivity and low-productivity participants with 95% confidence intervals in each round under cooperation and coordination (Figure 1b). In every treatment, high-productivity participants (HPP) contributed significantly more than low-productivity participants (LPP) (paired wilcoxon signed-rank tests: cooperation 1H: $P = 6.92 \times 10^{-7}$, $r = 0.696$ (95 % CI: [0.53, 0.83]); cooperation 2H: $P = 1.226 \times 10^{-5}$, $r = 0.613$ (95 % CI: [0.43, 0.77]); coordination 1H: $P = 4.622 \times 10^{-8}$, $r = 0.766$ (95 % CI: [0.64, 0.86]); coordination 2H: $P = 3.229 \times 10^{-4}$, $r = 0.504$ (95 % CI: [0.27, 0.70]); two-tailed). Allowing peer punishment markedly raised mean contributions (wilcoxon signed-rank tests, P rounds vs. NP rounds: Cooperation 1H: $P = 1.356 \times 10^{-13}$, $r = 0.733$ (95 % CI: [0.64, 0.81]); cooperation 2H: $P = 3.793 \times 10^{-12}$, $r = 0.688$ (95 % CI: [0.58, 0.78]); coordination 1H: $P = 7.032 \times 10^{-6}$, $r = 0.445$ (95 % CI: [0.30, 0.59]); coordination 2H: $P = 2.274 \times 10^{-5}$, $r = 0.420$ (95 % CI: [0.25, 0.58])). A comparison with the NP2 rounds ruled out order effects, confirming that peer punishment, not round order, drove the contributions increase, which was consistent with the previous research [44], that is, allowing participants to peer punishment can effectively promote the contributions. Also, the marginal impacts of peer punishment differed under cooperation and coordination. The increase of contributions under cooperation was significantly larger than that under coordination (cooperation: HPP $r = 0.721$ (95 % CI: [0.59, 0.82]), LPP $r = 0.718$ (95 % CI: [0.58, 0.81]); coordination: HPP $r = 0.456$ (95 % CI: [0.22, 0.66]), LPP $r = 0.578$ (95 % CI: [0.37, 0.74]); two-tailed). Moreover, the difference of contributions between HPP and LPP under cooperation was more significant than under coordination (cooperation P rounds: $r = 0.858$ (95 % CI: [0.75, 0.88]); NP rounds: $r = 0.869$ (95 % CI: [0.86, 0.87]); coordination P rounds: $r = 0.528$ (95 % CI: [0.10, 0.84]); NP rounds: $r = 0.668$ (95 % CI: [0.47, 0.81])). From the aforementioned results, we also found that the punishment-driven boost in cooperation is similar for both HPP and LPP, whereas in coordination the improvement is concentrated among LPP, sharply curtailing LPPs' free-riding.

As mentioned above, the effects of whether allowing peer punishment on behavioural factors in cooperation and coordination were indeed different. Does the relationship between punishments and contributions in P stage (rounds 22-36) also differ between cooperation and coordination? We quantified contribution behaviour index as each individual's total contributions and punishment behaviour index as (i) the total punishments a individual received and (ii) the total punishments a individual imposed in P stage. We found that the total punishments a individual received declined linearly with his total contributions (Figure 1c), which accorded with the intuition that peer punishment mainly targets free-riders. The negative slope was significantly steeper in coordination than in cooperation (cooperation: $p = 3.27 \times 10^{-13}$, $\beta_0 = -0.056$, 95 % CI: [-0.070,-0.042]; coordination: $p < 2 \times 10^{-16}$, $\beta_0 = -0.138$, 95 % CI: [-0.162,-0.115]). Remarkably, the total punishments a individual imposed also declined linearly with his total contributions. This contradicts the common view that high contributors, having invested more, are more willing to punish others. We argue that the pronounced prosociality of high contributors made them reluctant to punish. Consistent with the earlier pattern, this negative slope was again stronger in coordination than in cooperation (cooperation: $p = 3.93 \times 10^{-7}$, $\beta_0 = -0.040$, 95 % CI: [-0.055,-0.025]; coordination: $p = 1.36 \times 10^{-15}$, $\beta_0 = -0.114$, 95 % CI: [-0.141,-0.088]). Taken together, when individuals reduced their total contributions by the same amount, peer punishment was more severe under coordination than under cooperation. Actually, subsequent analyses (Section Conditional contribution patterns and conditional punishment patterns of cooperation-coordination) revealed that peer punishment in coordination was driven primarily by the punished individuals' own contributions (self-contribution coefficient), whereas in cooperation it was driven primarily by the recipients' contributions (recipient-contribution coefficient).

Finally, we classified the punishment factor at the dyadic level defined as paired punishment to further distinguish two types of punishment, namely the punishment of free-riding and the anti-social punishment. We used the difference between the punisher's and the recipient's contributions as the independent variable and showed the frequency of paired punishments for each deviation in a histogram (Figure **??**). Positive deviations were labelled punishment of free-riding, whereas non-positive deviations were anti-social punishment [45, 61]. Because only seven contribution options were available each round, decisions were highly discrete; consequently, most punishments occur when the deviation equals zero. We found that the proportion of anti-social punishment was lower in cooperation than in coordination (cooperation: $\theta = 0.4836$; coordination: $\theta = 0.5913$). Moreover, punishment was more likely to be anti-social when the group failed to reach the threshold in coordination (not reaching threshold: $\theta = 0.6249$; reaching threshold: $\theta = 0.5913$). We would elaborate on these patterns in the subsequent conditional punishment patterns analysis (Section Conditional contribution patterns and conditional punishment patterns of cooperation-coordination).

Overall, the model-free behaviour patterns in our experimental design replicated several established results and, more importantly, uncovered systematic differences in aggregate contribution behaviour between cooperation and coordination. By integrating common extensions in related research (namely, endowment heterogeneity and second-order norms governing peer punishment), we showed that coordination exhibited clearer contribution benchmarks and stricter norm-driven punishment than cooperation.

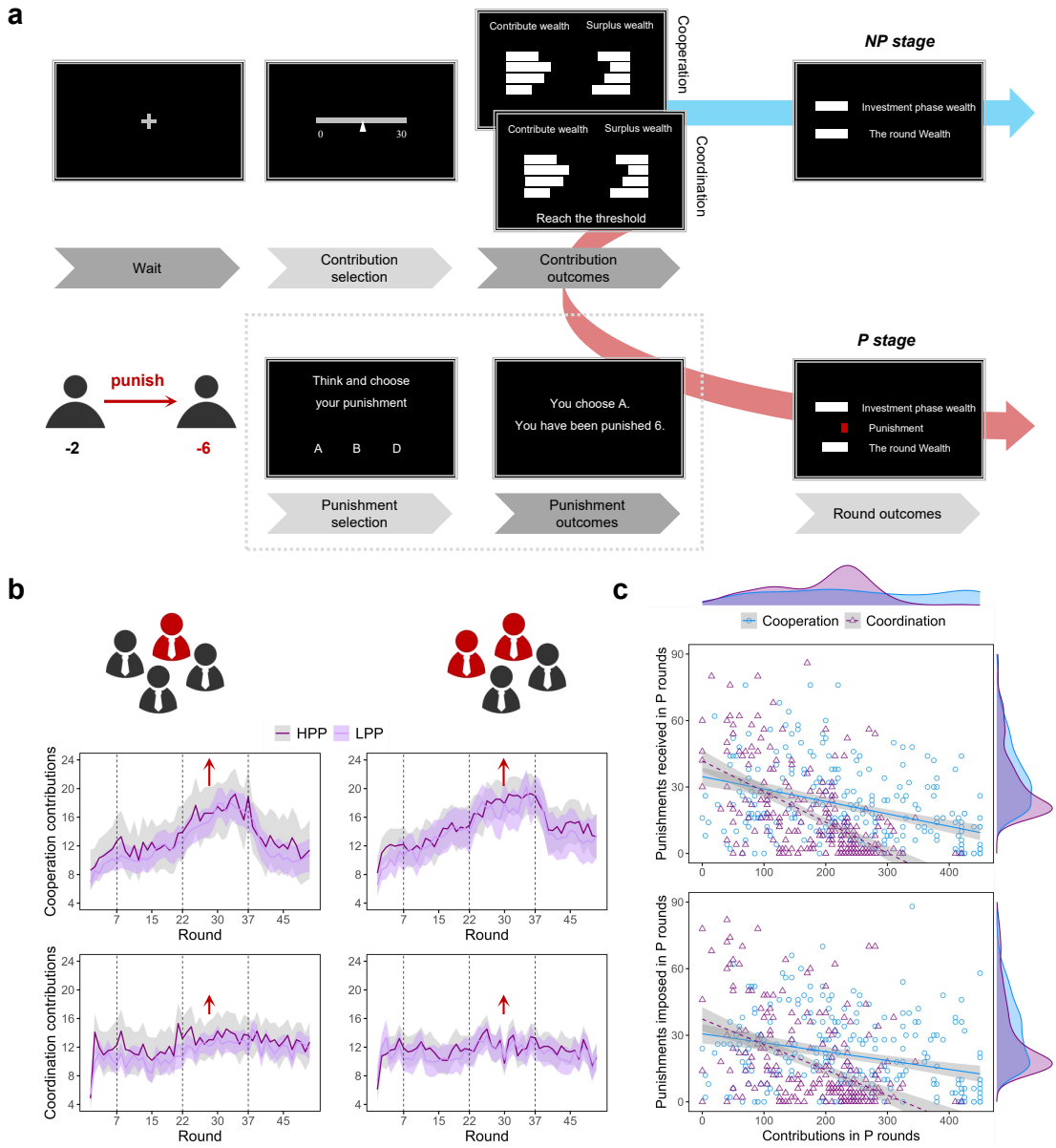

Fig. 1 Experimental procedure and model-free behaviour patterns. **a**, Schematic diagram of cooperation and coordination. After a brief gaze wait, participants firstly selected one of the seven contribution options and then observed the detailed contribution outcomes of the group. Next, in P stage, participants selected to punish the designated participants and then observed information regarding the total punishments they imposed and they received (indicated by the red guide arrow). In contrast, in NP stage, participants did not engage in punishment phase or observe any punishment-related information (indicated by the blue guide arrow). Finally, the screen displayed the final outcomes of the round. **b**, Mean contributions of cooperation and coordination across rounds. The line chart illustrates the mean contributions and 95% confidence interval made by high-productivity participants (HPPs) and low-productivity participants (LPPs), respectively. The dotted line indicates the four stages of the experiment: preparation rounds, NP1 rounds, P rounds, and NP2 rounds. The mean contributions of HPPs were higher than that of LPPs. Additionally, the mean contributions in P stage was higher than that in NP stage, regardless of cooperation or coordination. **c**, The linear relationship between total punishments and total contributions. In the scatter plot, the x-axis represents the total contributions, while the y-axis represents the total punishments received/imposed by participants in P stage. The histogram illustrates the respective distributions of punishments and contributions. Each point represents a participant, and the straight line indicates the linear regression result along with the 95% confidence interval. The two types of fitting slope between punishments and contributions in coordination were higher than that in cooperation.

Conditional contribution patterns and conditional punishment patterns of cooperation-coordination

A strategy is typically formalised as a probability vector over the space of past behaviour in game theory. [18, 62](see also introspection dynamics [63]). These strategies are usually inferred from the stable payoffs that are emerged after a sufficient number of group interactive rounds. Yet real decision-makers cannot precisely compute long-horizon payoffs, nor do they behave without noise or individual idiosyncrasy [33, 64]. Aiming at bridging this gap between strategic evolution and real behaviour, we therefore introduced the conditional behaviour patterns to capture the iterative feedback within group behaviour. Conditional behaviour patterns specify that the action taken in the current round is governed by the action observed in the preceding round (Figure 2a: conditional contribution patterns; Figure 2b: conditional punishment patterns). To account for the individual heterogeneity in decisions, we performed a Bayesian mixed recursive model. The model systematically calculated the distribution and uncertainty of parameters associated with different individuals' decisions, which are influenced by various factors. (see Method Individual-level analysis).

For the conditional contribution patterns, we first used the individual's own contributions and the total contributions of the other group members in the preceding round to predict the individual's contribution in the current round [18, 62]. Here the calculated coefficients were termed as stickiness and imitation, respectively [65]. A higher stickiness coefficient indicates rigidly sticking to own previous contribution decisions, whereas a higher imitation coefficient means decisions are flexible and highly imitative of others', often interpreted as a herd effect [38].

Separate regression analyses of contributions in NP and P stage for cooperation and coordination revealed that the coefficients were consistently positive across all four experimental conditions (Figure 2c, d). Regardless of round types, the stickiness coefficient was consistently higher under coordination than under cooperation (cooperation: $\beta^{NP}_{fixed} = 0.30$ (95% CI = [0.26,0.34]); $\beta^{P}_{fixed} = 0.38$ (95% CI = [0.33,0.44]); coordination: $\beta^{NP}_{fixed} = 0.38$ (95% CI = [0.34,0.42]); $\beta^{P}_{fixed} = 0.42$ (95% CI = [0.36,0.47])). Conversely, the imitation coefficient was always lower under coordination than under cooperation (cooperation: $\beta^{NP}_{fixed} = 0.43$ (95% CI = [0.39,0.46]); $\beta^{P}_{fixed} = 0.39$ (95% CI = [0.35,0.44]); coordination: $\beta^{NP}_{fixed} = 0.35$ (95% CI = [0.31,0.38]); $\beta^{P}_{fixed} = 0.34$ 95% CI = [0.29,0.38])). The patterns implied that individual behaviour was less susceptible to unexpected influence under coordination. Only with a more general consensus could participants clarify responsibilities, and thus exhibited greater stickiness [4, 15]. More importantly, allowing peer punishment markedly raised the stickiness coefficient under both cooperation and coordination (indicated by the red arrows in Figure 2d), demonstrating that second-order public goods reinforced producing consensus. Correspondingly, the imitation coefficient declined to varying degrees. Across all conditions, the significant negative correlation between the random slopes of stickiness and imitation across individuals meant that when the stickiness was high for a particular individual, the imitation tended to be low, and vice versa (see Figure **??**a,b) (cooperation: $r^{NP}_{random} = -0.73$ (95% CI = [-0.85,-0.59]); $r^{P}_{random} = -0.78$ (95% CI = [-0.92,-0.61]); coordination: $r^{NP}_{random} = -0.87$ (95% CI = [-0.93,-0.80]); $r^{P}_{random} = -0.79$ (95% CI = [-0.88,-0.67])). Replicating the analysis with corporate wealth (= contributions × productivity) yielded qualitatively identical relationship under cooperation and coordination (see Figure **??**).

For the conditional punishment patterns, we employed a generalized linear regression to analyse the binary dependent variable of whether an individual A punished a specified group member B (A punished B vs. A did not punish B). Motivated by the strategic nature of punishment, we included the recipient's contribution, the punisher's own contribution in the current round, and the punishment the punisher received in the preceding round (capturing anti-social retaliation) as regressors that

could affect the paired punishment. The corresponding coefficients were interpreted as the recipient-contribution, self-contribution, and retribution, respectively.

First, the retribution coefficient was significantly lower under cooperation than under coordination (Figure 2e) (cooperation: $\beta_{fixed} = 0.45$ (95% CI = [0.32,0.58]); coordination: $\beta_{fixed} = 0.76$ (95% CI = [0.60,0.93])), aligning with the model-free analysis (see Figure **??**). This explains why anti-social punishment was more prevalent under coordination than under cooperation: The higher tendency of individual retribution will directly lead to more common anti-social punishment. Second, we found the self-contribution coefficient was lower under cooperation than under coordination (cooperation: $\beta_{fixed} = 0.43$ (95% CI = [0.17,0.70]); coordination: $\beta_{fixed} = 0.69$ (95% CI = [0.40,0.90])). Conversely, the absolute value of the recipient-contribution coefficient was higher under cooperation than under coordination (cooperation: $\beta_{fixed} = -2.29$ (95% CI = [-2.56,-2.04]); coordination: $\beta_{fixed} = -1.90$ (95% CI = [-2.19,-1.64])). These patterns indicated that, under coordination, imposing punishment was driven primarily by a normative judgment of individual's own contribution, coupled with heightened retribution after being punished. Under cooperation, punishment instead targeted low contributions by the recipient. Finally, the correlation between the random slopes of recipient-contribution and self-contribution was negative across conditions similar to the conditional contribution patterns (see Figure **??**) (cooperation: $r_{random} = -0.63$ (95% CI = [-0.77,-0.45]); coordination: $r_{random} = -0.59$ (95% CI = [-0.74,-0.40])), revealing a stable psychological trade-off between these two determinants of punishment.

Beyond the level of behaviour patterns, we also examined how the conditional contribution dynamics, defined as the change in contributions between a specific round and the preceding round, were shaped by contextual factors (see Figure **??**a). In addition, we showed that punishment a individual received in P stage affected the individual's contribution dynamics rather than the contributions: after being punished, participants accelerated the growth of their contribution. We found that the $\Delta_{Imitation}$ coefficient was markedly higher under cooperation than under coordination across both NP and P stage (see Figure **??**b,c). Likewise, during P stage, the punishment coefficient was higher under cooperation than under coordination. These results aligned with the conditional contribution patterns and suggested that coordination promoted the stickiness of contribution dynamics that was not easy to change across rounds.

All the aforementioned conditional patterns demonstrated that individual behaviour was readily affected under cooperation, whereas individuals tended to stick to their own judgments under coordination, which established a qualitative framework in advance [15]. Under the consequentialist argument, the quality of cooperation was not clearly distinguished, resulting in flexible and variable individual contributions. In contrast, under the relational argument, it was easier to produce consensus within the group through coordination and the threshold. In the next section, we would further explain the psychological factors behind these patterns.

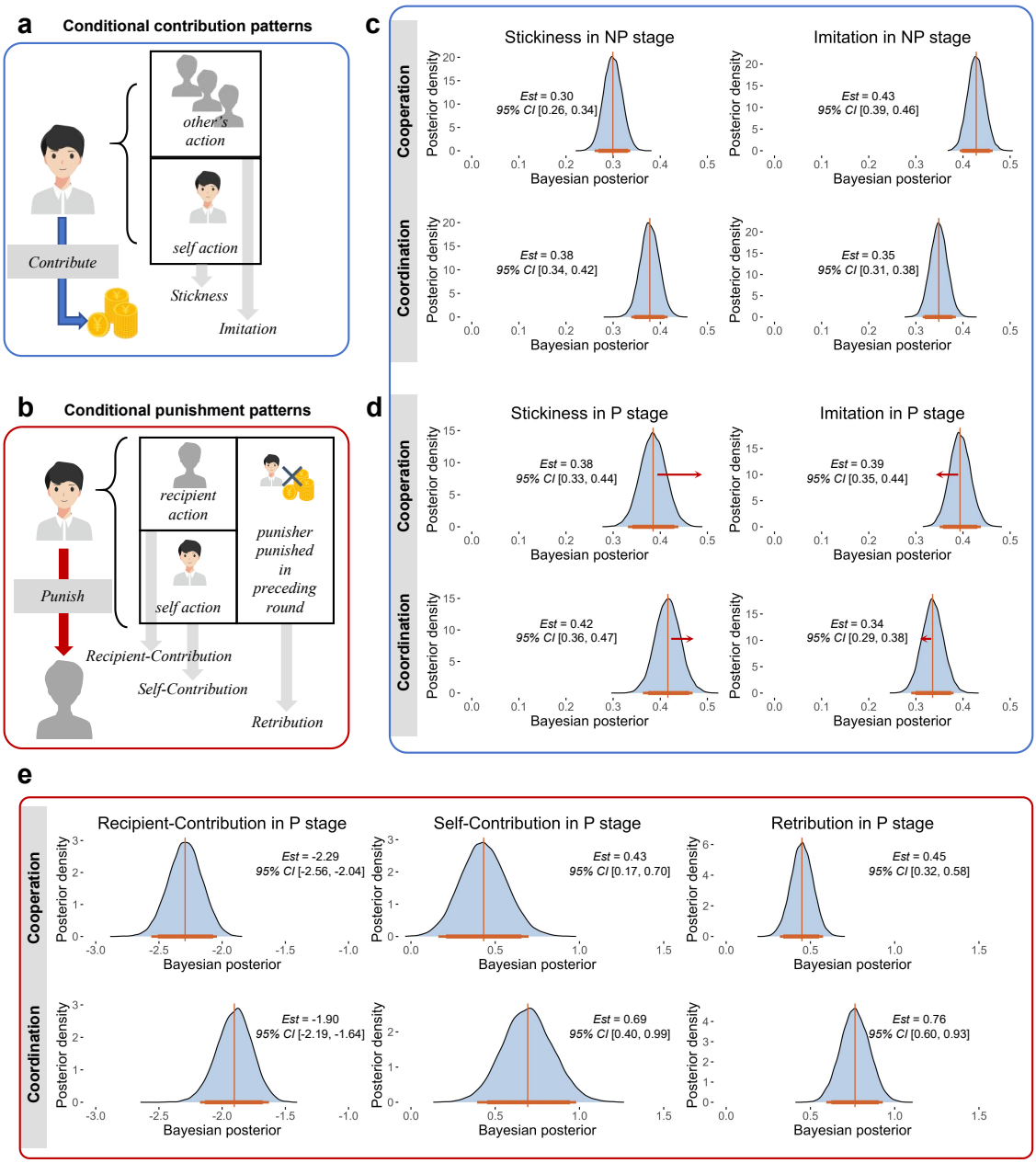

Fig. 2 The definitions and results of conditional behaviour patterns. **a**, Conditional contribution patterns setting. We referred to the previous related literature [32, 62, 65] and assumed that the individual's contributions in a certain round was influenced by the contributions of himself and others within group in the preceding round. **b**, Conditional punishment patterns setting. The individual's motivation to impose punishment was assumed to be affected by three factors: the contributions of the recipient, the individual's own contributions and the punishments the individual received in the preceding round. **c-e**, Bayesian posterior distributions of regression coefficients with the highest density interval (90%, 95%). The fixed effect of the stickiness coefficient in cooperation was lower than that under coordination, while the fixed effect of the imitation coefficient was higher than that under coordination. Compared with P stage (c), the stickiness coefficients of both cooperation and coordination in NP stage (d) was higher, while the imitation coefficients was lower. The fixed effect of the self-contribution coefficient and retribution coefficient under coordination was higher than that under cooperation, while the fixed effect of the recipient-contribution coefficient was lower than that under cooperation.

Psychological computation framework for cooperation and coordination

Thus far, we had analysed the differences of individual decision-making under cooperation and coordination from the perspectives of both model-free and conditional behavioural patterns. However, we still didn't know the differences of individual psychology caused by cooperation and coordination.

In this section, we will provide an interpretable psychological framework of cooperation and coordination. In order to prevent over-fitting caused by too many parameters, the utilities we considered were based on the contributions of investment phase. Instead, we considered the punishment phase as another kind of environment that affected individual psychology of contribution, and therefore we implemented fitting in NP1, P and NP2 rounds respectively.

In social interactions, decision-making is typically determined by the interplay of rationality and social norms [13]. On one hand, rationality exists in a world in which everyone always acts exclusively for his own selfish benefits. On the other hand, social norms also have a grip on the mind that is due to the strong emotions their violations can trigger. Therefore, we divided the motives of participants' contribution behaviour into rationality and social norms (For a detailed introduction of utilities, please refer to Method Psychological decision-making computational model), in which the calculation of rationality utilities were based on the expected contributions of other group members (Figure 3a). We defined the specified focal participant's estimation of expected contributions of other group members as the belief. As the round went on, each participant needed to track the contributions of others and predicted the contributions in the next round. We had applied two belief updating methods [10, 66]. The first one was reinforcement learning updating. By using Rescorla-Wagner rule, the historical beliefs tracked by participants were weighted with the expected errors obtained in the current round to update the beliefs. The second was Bayesian updating [67] based on normal distribution which not only gives estimated values, but also quantifies the uncertainty of estimation.

In this study, we adopted Elster's minimalist notions of rationality [13]. From the perspective of selfishness and unselfishness, motives were dichotomized into the self-regarding preference—concern for one's own payoff—and the social preference—concern for the payoffs of others, a distinction widely used in research about PGGs [28, 68]. Utility from social norms was modeled separately as the psychological cost incurred when one's contributions deviated from the prevailing group approvals. Following previous literature [41, 58, 69], this cost was implemented as an additive negative disturbance that applies only to contributions below the group's historical means. To prevent the overflow of the preparation rounds and respect limited memory, the historical window was set to the last two rounds ($t_0 = 2$).

Beyond the traditional self-interest utility framework, we specified six candidate models for cooperation and coordination by combining the weight structures and utility components described above (see Method The utility-based models). To keep the weighting scheme parsimonious, we normalized the self-regarding preference weight to 1 and treated it as the reference for all other utilities; this was reasonable because choice probabilities were ultimately generated via a softmax rule. For the social preference, we examined two specifications: (i) a fixed weight, and (ii) a variable weight that changed linearly with the expected contributions of others [68]. In the linear variant, the weight increased (positive slope) or decreased (negative slope) as the increase of expected contributions of others.

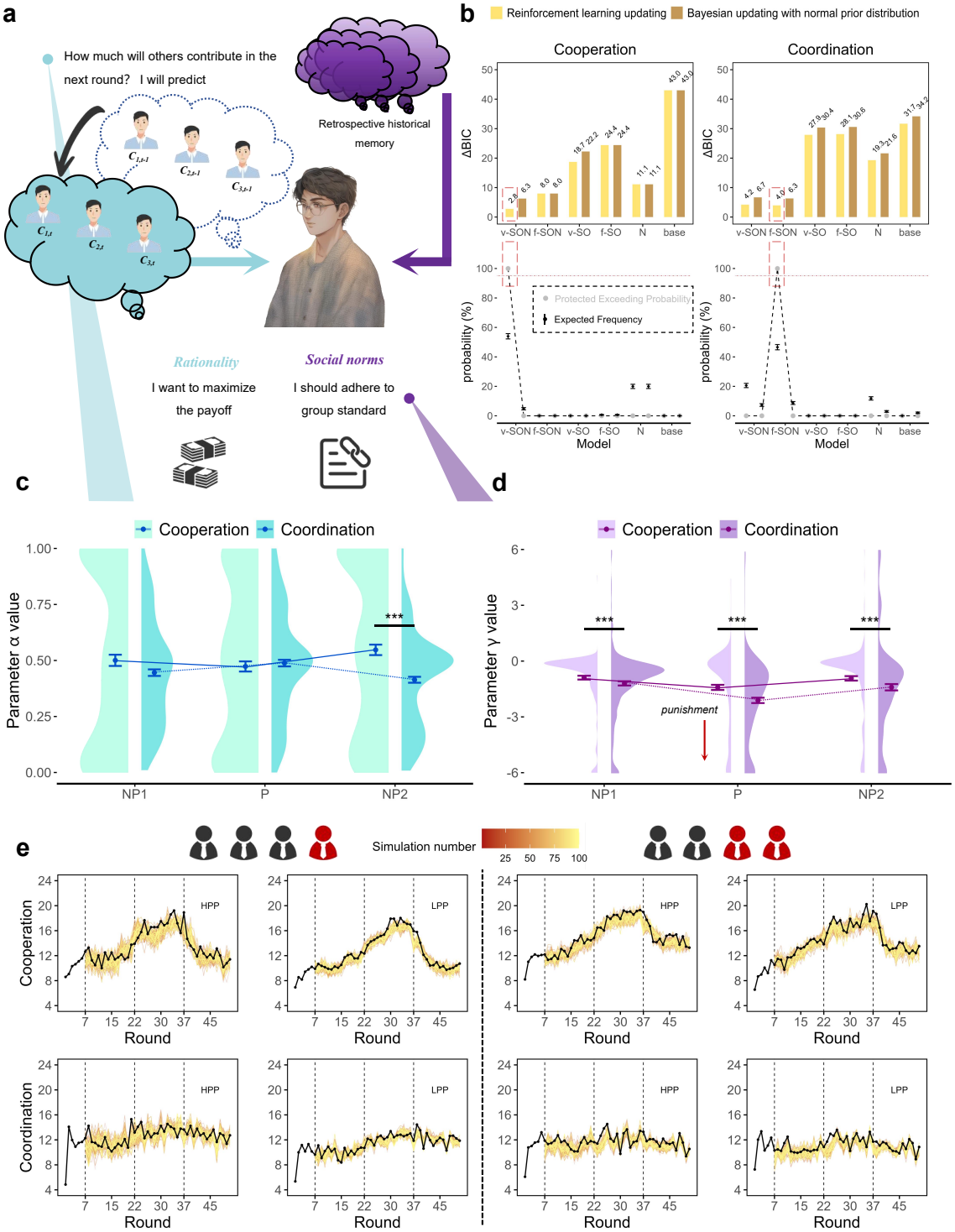

Fig. 3 Cooperation-coordination psychological computational framework and comparison of behaviour parameters of different mechanisms. **a**, Overview of SON model. Based on the stickiness and imitation, we classified the participants' behavioural motives into rationality and social norms [13], and the rationality utilities of self-regarding preferences and social preferences were based on predicting the contributions of others (see Figure **??**) [10, 28]. Social norms utility was defined as the psychological cost incurred due to the constraints of historical behaviour [41, 58]. **b**, Model selection. We calculated the ΔBIC of 12 models (2 update rules $\times$ 6 types of utility components) and two kinds of BMC standard values (expected frequency [EF] and protected exceedence probability [pEP]) [70] respectively. The red dotted line indicates that the threshold of probability (95%) is exceeded. The v-SON model won under cooperation, while the f-SON model won under coordination. **c-d**, Parameters distribution of winning model under cooperation and coordination. The distributions of learning rate parameter α are scattered in cooperation and concentrated around 0.5 in coordination (c). The distributions of social norms parameter γ are mainly below the X-axis, and it shows a clear decrease in P stage. Meanwhile, the absolute value of γ for coordination is significantly higher than that for cooperation, regardless of round types (d). **e**, mean contributions of different productivity participants after 100 simulations based on fitting model parameters.

Model fitting was assessed with the Bayesian Information Criterion (BIC). For each session we computed ΔBIC relative to the minimum BIC among the 12 models (six in cooperation or coordination). All reinforcement-learning updates decisively outperform Bayesian updating with a normal likelihood under identical components. Formal Bayesian Model Selection (BMS) identified the SON (Self-regarding, Others, and Norms) family as the most accurate model accounting for behaviour in cooperation and coordination. (Figure 3b: v-SON for cooperation and f-SON for coordination, each achieved a protected exceedance probability > 95%). Notably, the winning models differed in their required social preference weight: cooperation favored a dynamic, expectation-dependent weight, whereas coordination was best described by a fixed social preference weight. These findings provided compelling evidence that cooperative behaviour is highly flexible and influenced by the belief of others.

Both winning models (i) used reinforcement learning to track and predict others' contributions and (ii) combined the self-regarding and social preference utilities. In cooperation, the weight attached to social preferences increased significantly with the expected contributions of others (one-sample Wilcoxon tests, $\beta_{slope} : P = 0.0083, r = 0.095$ (95% CI = [0.02,0.17])). Thus, a higher contributions expectations of others in group would amplify the protective effect of social preferences on the public good [68]. Coordination showed no such sensitivity. The fixed component of social preferences was significantly positive under both cooperation and coordination (one-sample wilcoxon tests, cooperation:$\beta_{intercept} : P = 3.383e-06, r = 0.168$ (95% CI = [0.10,0.24]); Coordination:$\beta_{intercept} : P = 4.861e-13, r = 0.259$ (95% CI = [0.19,0.33])), indicating a baseline pro-social intentions in most cases [53](see also Figure **??**).

We next examined the two key parameters-the learning rate parameter α and social norms parameter γ (Figure 3c,d). Focusing on the transitions of adjacent round types, cooperation and coordination parameters α showed a clear divergence emerged between P and NP2 rounds-α increased significantly under cooperation (paired wilcoxon test, $P = 0.03895, r = 0.129$ (95% CI = [0.01,0.25])) and decreased significantly under coordination (paired wilcoxon test, $P = 4.37e-05, r = 0.253$ (95% CI = [0.14,0.37])). The social norms parameter was markedly lower in P rounds than in NP rounds under both cooperation and coordination (paired wilcoxon tests, cooperation:$NP1 \rightarrow P, P = 0.0285, r = 0.137$ (95% CI = [0.03,0.25]); $P \rightarrow NP2, P = 0.0002579, r = 0.228$ (95% CI = [0.10,0.35]); coordination:$NP1 \rightarrow P, P = 5.543e-07, r = 0.311$ (95% CI = [0.20,0.41]); $P \rightarrow NP2, P = 0.001303, r = 0.199$ (95% CI = [0.08,0.32])). These decreases confirmed that peer punishment, acting as a second-order public good, strengthened norm enforcement [41]. More importantly, we analysed the relationship between the parameters of cooperation and coordination in different round types. The absolute value of social norms parameter was consistently higher under coordination than under cooperation, regardless of the round types (wilcoxon tests, NP1:$P = 1.622e-08, r = 0.249$ (95% CI = [0.16,0.33]); P:$P = 2.15e-10, r = 0.280$ (95% CI = [0.20,0.36]); NP2:$P = 1.894e-10, r = 0.280$ (95% CI = [0.19,0.36])). The pattern indicated that coordination elicited more potent social norms than cooperation from a psychological perspective, mirroring the conditional behaviour patterns that coordination produced stronger consensus to avoid a huge psychological cost of deviating from approved behaviour. By NP2 rounds, learning-rate parameters stabilized, yet remained significantly higher under cooperation than under coordination (wilcoxon test, NP2:$P = 6.073e-05, r = 0.177$ (95% CI = [0.09,0.27])), meaning that participants needed to track the expected contributions of others faster and drive behaviour more flexibly under cooperation. This explained why imitation coefficient in cooperation was higher. Finally, we validated the model parameters (see Supplementary Section **??** and Figure **??**) and ran 100 simulations using the winning models and the fitted parameters (Figure 3e). The simulated trajectories closely reproduced the observed mean contributions,

demonstrating that the SON models and its specified utilities successfully captured the emergent dynamics of collective cooperation and coordination [66].

Neural activity of individual dmPFC and rTPJ

To capture individual-level neural responses, we analysed the time-series data of oxyhemoglobin concentration changes recorded via fNIRS throughout the experiment. First, we examined individual neural activation patterns in cooperation and coordination (see Section Intra-individual neural activation patterns for details). We observed significant differences in the right temporoparietal junction (rTPJ) channels activation under coopeartion and coordination. The mean activation of individual's rTPJ channels was significantly higher under coordination than under cooperation regardless of the round types (Figure 4b) (channel 5:$P = 9.55e-12, F(1,506) = 48.66, \eta_P^2 = 0.0877(95\%CI = [0.0478, 0.1345])$; channel 6:$P =< 2e-16, F(1,496) = 78.7, \eta_P^2 = 0.1369(95\%CI = [0.0908, 0.1886])$; channel 7:$P = 5.93e-06, F(1,505) = 20.95, \eta_P^2 = 0.0398(95\%CI = [0.0129, 0.0768])$; channel 8:$P = 1.23e-12, F(1,503) = 53.11, \eta_P^2 = 0.0955(95\%CI = [0.0510, 0.1466])$, all results remained significant after FDR correction). Focusing on the three channels exhibiting the most pronounced differences (channels 5, 6, and 8), we further tested their activation in investment phase across three round types (Figure 4c). Regardless of whether allowing punishment (NP or P stage), the mean activation in these channels were consistently and markedly different between coordination and cooperation. As a key node in the psychological network, rTPJ activation is modulated by the perceived sociality of the participant [71]. In our study, this perception was captured by the notion of "norms". That is, the group's consensus on contribution behaviour was stronger under coordination than under cooperation, which in turn drove a higher activation in rTPJ. However, during the punishment phase, no significant differences emerged in individual activation between cooperation and coordination (see Figure **??**). The finding is crucial, as it indicated that the neural fluctuations triggered by participants when enforcing second-order norms were minimal across cooperation and coordination.

We then used individual activation patterns to predict behaviour. We found that participants' mean contributions showed a significant positive correlation with the activation of rTPJ channel 5 during the investment phase under coordination, which did not emerged under cooperation (Figure 4d) (coordination:$\beta = 0.673(95\%CI = [0.221, 1.126]), P = 0.00372, t = 2.928$; cooperation:$\beta = 0.243(95\%CI = [-0.773, 1.260]), P = 0.638, t = 0.471$). The finding indicated that, under coordination, higher activation patterns reliably correspond to increased prosocial behaviour, whereas under cooperation the link between activation and behaviour remains weak. Simultaneously, the mean punishments the participant imposed displayed a significant positive correlation with the activation of rTPJ channel 5 during the punishment phase under both cooperation and coordination (Figure 4d) (cooperation:$\beta = 0.137(95\%CI = [0.047, 0.227]), P = 0.00289, t = 3.008$; coordination:$\beta = 0.141(95\%CI = [0.052, 0.231]), P = 0.0021, t = 3.108$). We assumed that the peer punishment behaviour, driven by similar intentions in both cooperation and coordination, was accompanied by pronounced neural fluctuations [72], indicating that a higher individual activation predicted a stronger intention to regulate group behaviour. Likewise, at the round level, rTPJ channel 5 remained positively correlated with the mean contributions under coordination ($\beta = 0.167(95\%CI = [0.057, 0.276]), P = 0.00375, t = 3.065$, see Figure **??**), whereas the correlation was absent under cooperation.

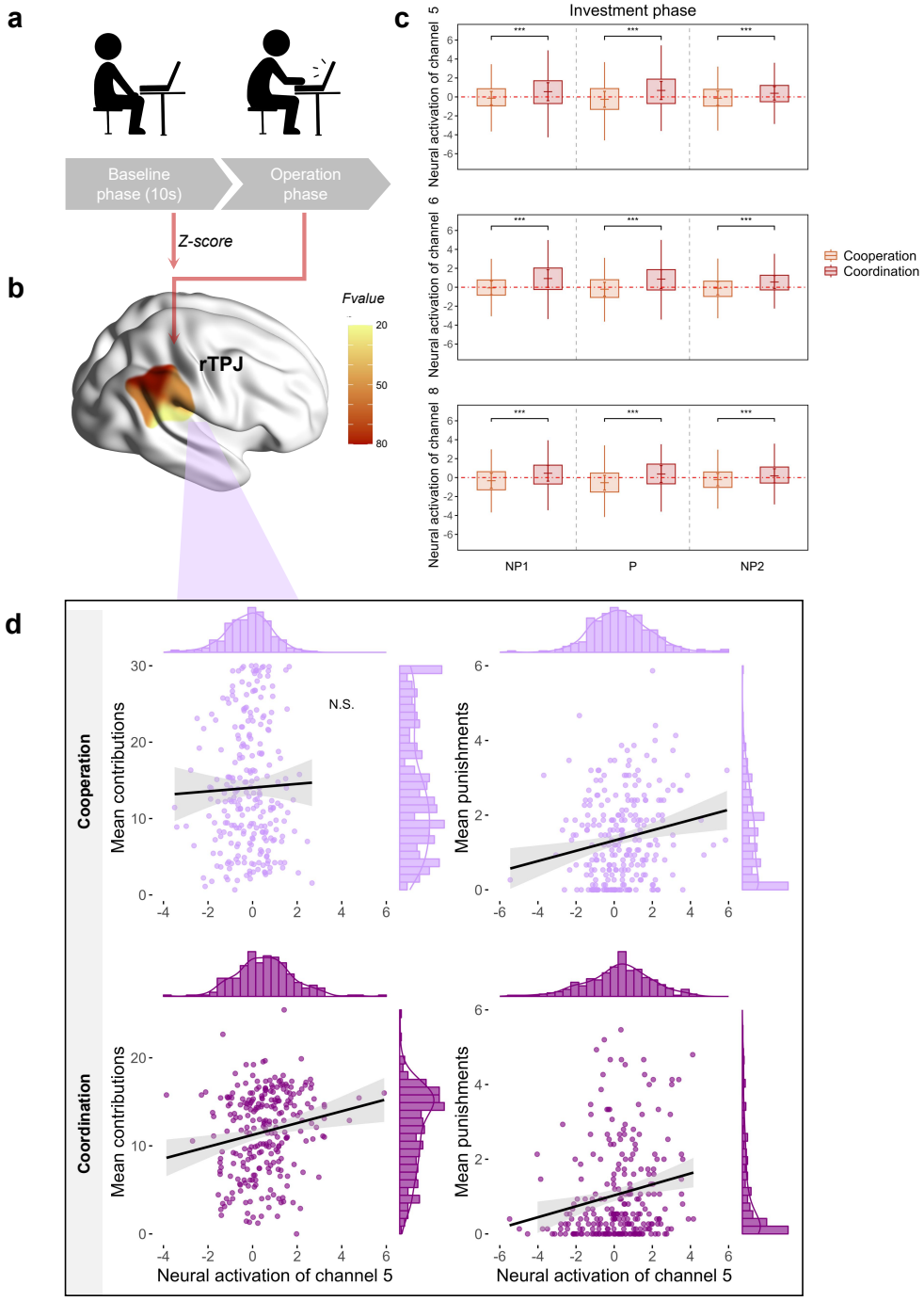

Fig. 4 Neural activation patterns and the relationship with behaviour. **a**, Neural activation calculation method. The 10 s before the operation phase served as the baseline. Z-score transformation of neural data during the operation phase was conducted using the baseline mean and standard deviation. **b**, The differences of individual neural activation across all rounds between cooperation and coordination. The channel differences in the rTPJ were significant (all channels were $P < 10^{-5}$, corrected by FDR). **c**, The differences of individual neural activation between cooperation and coordination during the investment phase in NP1, P, and NP2 rounds. We selected rTPJ channels 5, 6, and 8, which exhibited pronounced activation differences. The neural activation under coordination was significantly higher than that under cooperation. **d**, The relationship between individual behaviour in operation phase and neural activation. The mean punishments imposed by individuals under both cooperation and coordination were positively correlated with neural activation (right panel). However, there was a significant positive correlation between the mean contributions of individuals and neural activation under coordination, but there is no such phenomenon under cooperation (left panel).

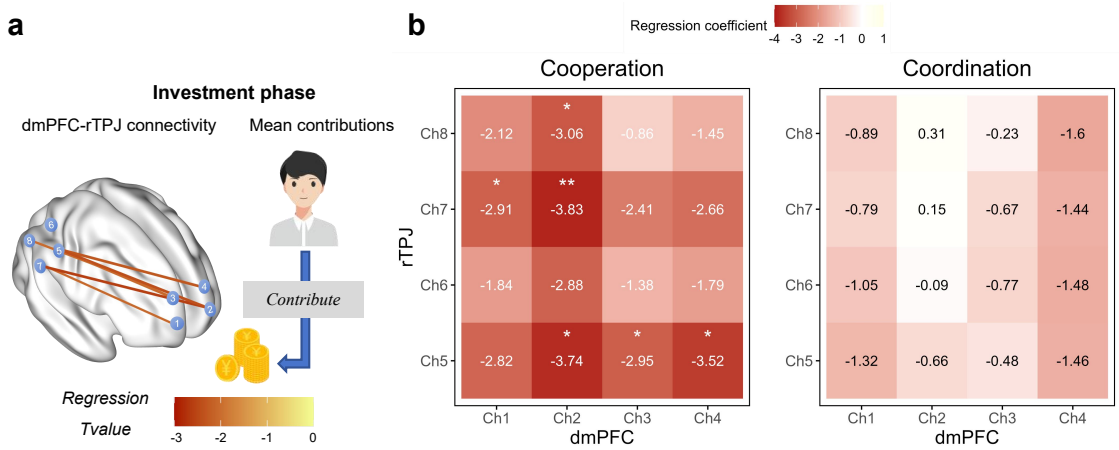

Fig. 5 The relationship between neural functional connectivity and behaviour. **a-b**, The linear relationship between dmPFC-rTPJ coherence and mean contributions under cooperation. The connectivity line indicated a significant regression coefficient, with the color of the connectivity line representing the t-value (a). The surviving dmPFC-rTPJ channels exhibited a negative correlation between coherence and mean contributions. Under coordination, the relationship between the two variables was not significant in any channel (b).

We also assessed individual functional connectivity by quantifying the coherence between dmPFC–rTPJ channel pairs, using the coherence as the pair-wise index of functional coupling (see Section Neural functional connectivity patterns for details). We examined the correlation between participants' the functional connectivity of distinct dmPFC–rTPJ channel pairs and mean contributions (Figure 5a) and observed a significant negative linear relationship between two variables under cooperation, whereas no such relationship emerged under coordination (Figure 5b) (cooperation: channel 1-7:$\beta = -2.906(95\%CI = [-5.641, -0.172]), P = 0.0374, t = -2.093$; channel 2-5:$\beta = -3.743(95\%CI = [-6.826, -0.660]), P = 0.0175, t = -2.391$; channel 2-7:$\beta = -3.833(95\%CI = [-6.729, -0.937]), P = 0.00968, t = -2.607$; channel 2-8:$\beta = -3.061(95\%CI = [-6.033, -0.089]), P = 0.0436, t = -2.028$; channel3-5:$\beta = -2.951(95\%CI = [-5.797, -0.105]), P = 0.0422, t = -2.042$; channel 4-5:$\beta = -3.524(95\%CI = [-6.561, -0.487]), P = 0.0231, t = -2.286$). The result is intriguing: the higher a participant's dmPFC–rTPJ functional connectivity during investment phase, the lower his total contributions. This counter-intuitive pattern could be interpreted as "rational selfishness"; the elevated connectivity likely reflected deliberate, reflective processing in which individuals forecasted the contributions of group members and then strategically withheld their own wealth [73]. Because the Nash equilibrium of cooperation is unique—zero contribution for all, that is, the optimal strategy for each individual is to contribute nothing. When functional connectivity between dmPFC and rTPJ was high, this rational deliberation drove contributions downward; conversely, weaker connectivity favored an intuitive response that promoting cooperation [73]. Under coordination, rational selections did not necessarily imply zero contribution, because withholding contributions might lower participants' payoffs relative to the extra wealth obtained once the threshold was reached (see Supplementary Section **??** for details); consequently, the negative correlation observed between dmPFC–rTPJ connectivity and mean contributions did not emerge.

In summary, the distinct behavioural and neural signatures observed under cooperation versus coordination can be understood within a unified psychological framework. In this account, coordination fosters a more robust social consensus among participants, manifesting as heightened activation in the rTPJ, whereas cooperative behaviour is more flexible and changeable, corresponding to lower

rTPJ engagement. However, contributions in cooperation exhibited a pronounced balance of intuition and reflection: the more rationally participants deliberate, the less they contribute, which was evidenced at the neural level by the negative correlation between dmPFC–rTPJ connectivity and contributions.

Differences of inter-brain neural synchronization between cooperation and coordination

While single-brain responses provided a fundamental understanding into individual psychological processes, social decision-making might also implicate coherent activity patterns across multiple brains as a deeper substrate underlying the distinctive features of interactive behaviour. In this study, we employed wavelet transform coherence (WTC) to quantify such inter-brain coherence, subtracting the resting-state values from those obtained during the resting baseline (see Section Inter-individual neural synchronization patterns), thereby defining the inter-brain neural synchronization (INS) patterns (Figure 6a). First, we identified the channels in which inter-brain synchronization during the investment phase exceeded that during the resting baseline. Synchronization was significantly enhanced in rTPJ channel 5 under cooperation, whereas it was observed in dmPFC channel 2 and rTPJ channel 5, 6 under coordination (Figure 6b, cooperation: channel $5 P = 0.007206, t(63) = 2.778, Cohen' sd = 0.347$ (95% CI = [0.097,0.597]); coordination: channel $2 P = 0.003384, t(63) = 3.046, Cohen' sd = 0.456$ (95% CI = [0.131,0.631]); channel $5 P = 0.003914, t(63) = 2.996, Cohen' sd = 0.381$ (95% CI = [0.125,0.624]); channel $6 P = 0.02164, t(63) = 2.3552, Cohen' sd = 0.306$ (95% CI = [0.045,0.544]), all channels survived FDR correction). Next, we compared the INS patterns of dmPFC channel 2 of all three round types between cooperation and coordination. The synchronization strength under coordination was significantly higher than under cooperation ($P = 0.00462, F(1, 382) = 8.119, \eta_P^2 = 0.0208$ (95% CI = [0.0023,0.0527])). We conducted 1000 pseudo-group permutation tests for both cooperation and coordination (Figure 6c). The significant enhancement of INS synchronization for channel 2 under coordination survived the permutation test ($P = 0.000$), and the difference in INS patterns of channel 2 between cooperation and coordination was also specific to the real group ($P = 0.015$). We concluded that the differences in INS patterns in dmPFC between cooperation and coordination indicated that groups have a stronger capacity to share intentions and goals under coordination [74]. In previous literature, the dmPFC has also been considered to play an important role in social interaction intentions and participates in expressing others' intentions [51, 71]. Additionally, the rTPJ channels failed the permutation test (see Figure **??**). In fact, for rTPJ channel 5, the INS patterns under both cooperation and coordination might be driven by the experimental task eliciting similar neural fluctuations across participants.

Next, we examined the relationship between overall INS and behaviour. Based on the aforementioned analysis, we averaged the INS in dmPFC channels. The behavioural interactive factors we selected were the cosine similarity of contribution vector pairs in round order and the paired mutual punishment (the total amount of punishment wasted by peer punishment). We found that the cosine similarity of contribution vector pairs was negatively correlated with the INS under coordination, which indicated that individuals within the group tended to reduce their contributions as the contributions of others increased [75](Figure 6e, $\beta = -0.162(95\% CI = [-0.306, -0.018]), P = 0.028, t = -2.206$), while mutual punishment was positively correlated with the INS ($\beta = 66.249(95\% CI = [20.588, 111.909]), P = 0.00457, t = 2.853$). However, the aforementioned significant linear relationships was not observed under cooperation due to the absence of a clear, threshold-like goal as seen in coordination (see Figure **??**, behaviour similarity: $\beta = -0.084(95\% CI = [-0.240, 0.072]), P = 0.291, t = -1.058$; mutual punishment:$\beta = -23.224(95\% CI = [-67.000, 20.552]), P = 0.298, t =$

−1.043). These findings not only revealed the underlying reasons for the intriguing negative correlation between multi-brain synchronization and behaviour, but also offered more intuitive neural evidence that coordination can foster stricter social norms and consensus within groups compared to flexible cooperation.

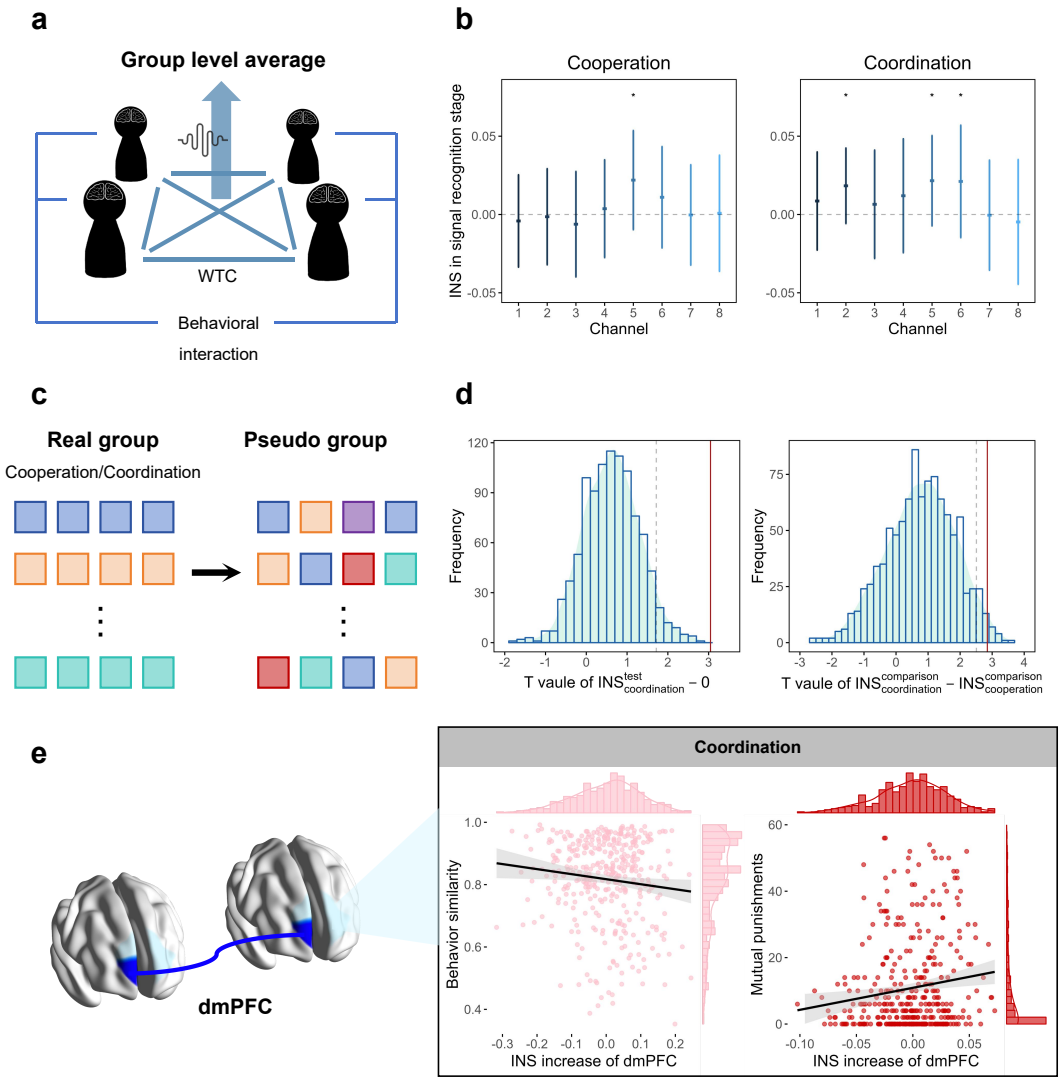

Fig. 6 Neural INS patterns and the relationship with behaviour. **a**, Acquisition of group INS and the correlation method between INS and behaviour. We calculated the WTC values for each pair of four participants and averaged the six WTC values to obtain INS. **b**, INS significant channels identification. We found that channel 5 of the rTPJ survived under both cooperation and coordination, while channel 2 of the dmPFC and channel 6 of the rTPJ survived under coordination. **c**, Pseudo-group test method. Because pairwise pairing was involved, our generation method ensured that no two participants in the same real group are assigned to the same pseudo-group. **d**, Pseudo-group test results. We generated 1,000 pseudo-groups under cooperation and coordination to test whether the significance of dmPFC channel 2 differed between cooperation and coordination. The real group t-value exceeded the 95% threshold under the permutation test, indicating that group channel 2 was significantly synchronized under coordination and that INS was significantly higher under coordination than under cooperation. **e**, The relationship between the overall mean of dmPFC INS and behavioural interactive factors under coordination. There was a significant negative correlation between the cosine contribution behaviour similarity and INS, but the phenomenon did not appear under cooperation. However, there was a significant positive correlation between the total amount of mutual punishment and INS under cooperation and coordination.

Discussion

Cooperation and coordination are two basic mechanisms to promote the welfare of human society. Nevertheless, the fundamental differences between cooperation and coordination in behaviour and psychology are remain unclear. Here, we designed an experimental paradigm based on two types of PGGs to systematically elucidate the nature of these two mechanisms. We expanded the range of contribution options available to participants [30], which allowed for a more accurate reflection of their behavioural intentions compared to the traditional binary selections. Also, we utilized a multi-brain framework that all participants actively engaged in decision-making, avoiding potential confounds and trust change from human-machine interactions [10, 28, 76]. In addition, our study incorporated key factors including second-order public goods punishment and productivity heterogeneity that were of significant interest in evolutionary game theory and behavioural economics. Specifically, we employed both intra-subject factors (i.e., NP stage and P stage) and inter-subject factors (i.e., 2HPP and 1HPP). These factors were examined under varying degrees of productivity heterogeneity within cooperation and coordination, thereby providing a comprehensive framework for understanding the underlying dynamics of decision-making.

Our results revealed that allowing peer punishment could significantly enhance the enthusiasm for contributing to the welfare of the group. However, the additional NP2 rounds indicated that this effect was not sustainable. Once the punishment constraint was removed, individuals' contribution enthusiasm reverted to its original level. More importantly, our results demonstrated that the promotional effect of peer punishment on coordination was weaker than on cooperation. We found that under coordination this type of imposed second-order public goods primarily enhanced the success rate of groups in high threshold and medium threshold, which were more difficult tasks. However, it did not significantly affect the success rate for relatively easier tasks. When peer punishment was permitted, individuals who contributed less tended to receive and impose more total punishments. The former finding—that those who contributed less, often labeled as selfish individuals, were more likely to be punished—was consistent with intuitive expectations. In contrast, the latter observation, that low-contribution individuals also imposed more punishment, stemmed from a retaliatory motive that individuals with a lower prosocial nature viewed punishment as a means of counterattack [61]. These findings indicated that individuals were more sensitive to the total contributions under coordination compared to cooperation. Additionally, the frequency of anti-social punishment was higher under coordination than under cooperation. Prior research had suggested that productivity heterogeneity did not lead to significant differences in participants' contributions [21, 23]. However, our study revealed that under both cooperation and coordination, individuals exhibited an attitude akin to "with great power comes great responsibility". The mean contributions of high-productivity participants were significantly higher than that of low-productivity participants, regardless of whether peer punishment was permitted. This phenomenon was particularly pronounced under cooperation. We further conducted simulations and found that the variation in group size might be the reasons underlying these contradictory findings (see Supplementary Section **??** for details). The high-productivity attribute was particularly pronounced in four-person groups, especially in the 1HPP (one high-productivity participant) setting.

We also established a unified analytical framework that integrated different mechanisms and behavioural factors. We employed the Bayesian mixed recursive model to define the conditional behaviour patterns. We found that the decision-making of group members was more consensus under coordination, whereas it was more flexible and lacks persistence under cooperation for the lack of a clear goal. Allowing peer punishment mitigated the flexibility to some extent. In addition, whether imposing punishment under cooperation was based on the contributions of others, whereas under

coordination, their own contributions served as the standard. The heightened sensitivity to group consensus under coordination and the general flexibility of behaviour under cooperation indicated that individuals might be driven by different psychological motives.

We further developed computational models to compare and unveil the underlying psychological mechanisms that drove the behavioural patterns we observed. The model distinguished the two fundamental utilities: rationality and social norms. Rationality represented the tendency of individuals to maximize their expected payoffs. Through the process of reinforcement learning, individuals predicted the benefits of different behaviour based on the updated behavioural belief of others. The social norms were mandatory expectations that focused on what individuals should do. Norms defined here are similar to rule-rationality [77] and dynamically evolves in the model based on historical behaviour. Consistent with prior literature, allowing peer punishment did enhance the binding role of social norms [41]. Importantly, we found that individuals' compliance with social norms was consistently stronger under coordination than under cooperation, regardless of whether peer punishment was permitted or not. This result confirmed the qualitative discovery of contribution behaviour from the perspective of psychological utility and further clarified the reasons for a clearer normative consensus under coordination. We also found that individuals under cooperation maintained a high learning rate when their decision-making tendencies were stable. This phenomenon might be related to the consequentialist orientation [15], which requires individuals to continuously update the group's identity behaviour.

Based on the hyperscanning method, we could intuitively compare the different neural reactions elicited by cooperation and coordination. First of all, in the investment phase, the rTPJ was activated more significantly under coordination than under cooperation, whereas such difference was insignificant in the punishment phase. Meanwhile, the general activation of the rTPJ was more pronounced in the punishment phase than in the investment phase. The reasons underlying these differences were distinct. The heightened attention to the threshold goal and the stronger consensus within the group led to more pronounced rTPJ neural fluctuations under coordination. In contrast, during the punishment phase, individuals experienced strong negative emotions, resulting in a generally higher activation compared to that observed in the investment phase. It is worth noting that the activation of the rTPJ under coordination could effectively predict both contributions and punishments, whereas under cooperation it could only predict punishment behaviour. These provided evidence that the rTPJ, a key region for perceiving group consensus [36], was significantly activated under coordination with stricter social norms, and its activation pattern could effectively correspond with behaviour only when strongly pronounced. Secondly, the behavioural prediction by neural response were opposite in the dmPFC-rTPJ functional connectivity pattern. The coherence was significantly enhanced with the decrease of contributions under cooperation, while no similar relationship was found under coordination. In fact, the increasing neural network linking these two brain regions activity leads to the calculated greed [73] associated with rational individuals, thereby reducing their contributions. Finally, we showed that the INS patterns of the rTPJ under both cooperation and coordination were remarkably synchronized. However, this notable synchronization was not specific to the group. Individuals exhibited significantly higher synchronization in the dmPFC under coordination than under cooperation. In addition, the higher overall INS of the dmPFC could effectively predict total mutual punishments and behavioural similarity under coordination. This indicated that the INS pattern further reflected the mutual recognition of complex group decision-making and the relationship between the complementarity of contribution behaviour and the brain synchronization index under coordination, whereas there was no relevant phenomenon under flexible cooperation.

Overall, our research systematically reveals the fundamental differences between cooperation and coordination at multi-scale levels, which firstly analysed the similarities and differences in behavioural and psychological representations, and then clarified the motives elicited by the neural responses. Our research can provide valuable insights into the understanding of reciprocal behaviour and a more in-depth elucidation and exploration of social interactions. Also, our research holds extensive applications. On one hand, our experimental paradigms can be extended to various decision-making scenarios [53], offering methodological support for unlocking the mystery of reciprocal behaviour in modern society [78]. On the other hand, the mechanistic insights into these two basic mechanisms provide a theoretical foundation for designing targeted incentive schemes that promote more efficient reciprocal behaviour, which is helpful to solve some major social challenges like climate change, energy sustainability and social inequality [79].

Undeniably, our research also has some room for expansion in the future. First, our paradigm currently employed discrete options, specifically a seven-level options, to facilitate robust data fitting. Future work could expand this approach to encompass a broader decision-making space, like continuous decision-making which has been found to drive stable and smooth behaviour [80, 81]. Second, in our experiment, we did not account for the nonlinear high-order interactions that may be present in multi-person interactions, which have been shown to be prevalent in contagion and other scenarios [82–85]. Future studies could examine the distinct properties exhibited by the two mechanisms under higher-order and pairwise interactions. Third, investigating the impact of human-machine hybrid systems on human cooperation and coordination, as well as the design of collaborative AI, represents a meaningful and promising direction for future research [86, 87].

Methods

Participants

We performed G*power to determine the sample size [88]. To ensure adequate statistical power for detecting behavioural and neural dimension differences between cooperation and coordination, we employed a fixed-effects ANOVA model to estimate the required sample size. For a two-group comparison, we set the effect size $f = 0.3$, significance level $\alpha = 0.05$, and desired statistical power $1 - \beta = 0.9$. These parameters yielded a required total sample size of 120.

We recruited 536 undergraduate participants from Beihang University. Five groups (20 participants) were excluded due to failure to arrive on time, inability to understand the procedure, or accidental withdrawal during the experiment. Ultimately, 516 participants (129 groups, 264 females, aged 17 - 25) remained for behavioural analysis. All participants received cash rewards ($12 - 20) based on experimental performance. One group was excluded from neural analysis due to fNIRS recording issues, leaving 512 participants (128 groups) for neural analysis. This met the sample size requirement estimated by G*power.

All analysed participants were right-handed, with normal or corrected-to-normal vision, possessed basic computational skills, and completed control problems. The experiment was approved by the Beihang University Biomedical Ethics Committee (protocol no. BM20250183). Written informed consents were obtained from all participants before the task. The study adhered to the Declaration of Helsinki and other relevant international ethical guidelines to ensure the safety and well-being of participants.

The heterogeneous public goods game paradigm consists of three distinct stages

The task of our design was a three-stage public goods game (PGG) experiment based on a heterogeneous productivity setting. In each group of four participants, one or two individuals was set a high productivity (=3.2), while the others were set a low productivity (=1.6). Each participant decided the points to contribute, ranging from 0 to 30 points. The contributions were multiplied by each participant's productivity and summed to form the public pool. The public pool wealth was equally distributed among the four participants and then received their retained wealth plus their share from the pool under cooperation. while under coordination , the public pool wealth was compared to a pre-set threshold. If it met or exceeded the threshold, participants received their retained wealth plus an equal share of the threshold amount; otherwise, they only received their retained wealth. For detailed calculations, see Method The components of utility.

Experimental procedure

The experimental procedure consisted of three sequential processes: preliminary preparation, the main experiment, and a post-experiment survey. Each experiment lasts about 100min.

Preliminary preparation

The day before the main experiment, registered participants were invited to a designated location to complete the pre-experiment questionnaire. The pre-experiment questionnaire screened participants for eligibility and collected background data needed for subsequent analyses (see Figure **??**). The questionnaire collected participants' basic personal information, incentive economic preference measures and social value orientation(SVO). Basic personal information included age, gender and subject background. The incentive economic preference measured [89] elicited participants' behaviour preferences, including risk aversion, patience, trust, altruism and positive and negative reciprocity, by asking them to make choices in a series of realistic decision scenarios. Social value orientation was assessed with the SVO slider task [90], which gauged participants' motives for allocating resources between themselves and others and then derived their value orientation. Eligible participants read the experimental instructions and then signed an informed-consent form; they were also reminded that participation was permitted to participate experiment only once.

Main experiment

Participants were evenly assigned to one of four between-group conditions defined by a 2 (cooperation vs. coordination) $\times$ 2 (two high-productivity participants [2HPP] vs. one high-productivity participant [1HPP]) factorial design; each participant's productivity remained fixed throughout the experiment. The experimental task was introduced via on-screen instructions and synchronized voice broadcast. The experimental task was framed as an investment in a virtual company. Each participant was randomly assigned a fixed identity label—A, B, C, or D—that remained unchanged throughout the experiment. To prevent reputational concerns from influencing decisions, identity codes were anonymized and permanently dissociated from participants' real identities; moreover, no participant ever learned which code corresponded to any other group member. Participants were instructed to remain silent throughout the experiment, view only their own computer screens, and refrain from observing either other participants or their displays. To minimize motion-related artefacts in the neural recordings, participants were instructed to hold the mouse with their right hand and rest their left

hand on the table throughout the experiment. Keyboard use was prohibited throughout the experiment; participants moved and clicked the mouse only during the operation phase, and remained motionless during all inter-trial rest periods.

To prevent confusion about the PGG procedure from biasing participants' behaviour, we referred to the research [91, 92] and designed three sets of control questions that mapped each round's contributions and punishments to their corresponding outcomes (see Section **??**). The experiment began only after all participants had answered the control questions correctly. After all the participants answered the control questions, the subjects wore fNIRS equipment for the participants.

Before the formal experiment began, participants were instructed to remain still for a 120-s resting baseline fNIRS recording. In the formal experiment, participants completed 51 decision-making rounds: The core experiment was divided into four stages: The first stage (preparation rounds, rounds 1–6), the second stage (NP1 rounds, rounds 7–21) and the fourth stage (NP2 rounds, rounds 37–51) were identical, ending immediately after participants made their contributions. The third stage (P rounds, rounds 22–36) allowed peer punishment, where participants could punish others based on their contributions by sacrificing 2 points of their own wealth to deduct 6 points from the designated participant. To avoid end-game effects, participants were never told the total number of rounds, and no round counter appeared on-screen [21].

In the P rounds of cooperation, participants first viewed a 5-s fixation cross signaling the imminent beginning of the round. Next entered the investment phase. Participants first deliberated on their contribution selection for 5 s, then used a horizontal slider (0–30 points, with a scale for every 5 points) to select their contributions within 7 s. After a 2–3 s pause (during which the system calculated and logged the interaction outcomes), the investment results appeared for 10 s, displaying each participant's productivity, contributed wealth, corporate wealth (contribution × productivity), surplus wealth, and final wealth. To maximize clarity and rapid comprehension, results were presented as combined bar-and-number displays, with each participant's own data highlighted in the top row of every on-screen module. Participants then deliberated on their punishment decision for 5 s and, within the next 7 s, used the mouse to designate whom to punish. Upon selecting a letter, the corresponding box turned red, signifying that the associated participant was being punished. Following a 2–3 s interval, during which the screen displayed the number of punished participants and the amount of wealth sacrificed for punishment, the investment and punishment phases of the round concluded. The round final outcome then appeared for 7 s, showing the participant's own investment wealth, any wealth lost through punishment received, and the resulting final wealth for the round. To prevent direct reciprocity, punishment remained fully anonymous: participants never saw who had punished them. A 10-s rest separated successive rounds. NP rounds followed the same sequence as P rounds, but omitted the punishment phase. After the investment results were shown (10 s), the final outcome was displayed immediately (7 s), with the "wealth lost to punishment" field set to zero.

In the P rounds of coordination, during the investment phase, while participants deliberated and selected their contributions (5 s + 7 s), the round threshold was shown at the bottom of the screen. Likewise, in the subsequent 10-s outcome display, the screen indicated whether the corporate wealth had met or exceeded that threshold. In addition, the experimental process of coordination was the same as that of cooperation. For setting the threshold, we defined three threshold levels. The high threshold corresponded to the corporate wealth if all members contributed 20 of their 30 points: 192 points under the 2-high-productivity (2H) setting and 160 points under the 1-high-productivity (1H) setting. The middle threshold corresponded to the corporate wealth if all members contributed 15 of their 30 points: 144 points under the 2H setting and 120 points under the 1H setting. The low threshold corresponded to the corporate wealth if all members contributed 10 of their 30 points: 96

points under the 2H setting and 80 points under the 1H setting. Each threshold type—high, middle, and low—was presented equally often across the experimental stages: twice in the preparation rounds and five times each in NP1, P, and NP2 rounds. Within each stage the order was fully randomised. Moreover, to introduce unpredictability, every threshold was independently jittered: with probability 0.25 it was increased by 8 points and with probability 0.25 it was decreased by 8 points; otherwise it remained unchanged.

Post-experiment survey

The post-experiment questionnaire was designed to assess participants' behavioural and cognitive changes across the entire study and to collect detailed feedback on the main task (see Section **??**). The questionnaire assessed participants' expected contributions, perceived task fit across NP and P stages, and the motivations behind their contribution and punishment decisions. Specifically, participants indicated the amounts they believed high-productivity and low-productivity participans ought to contribute and stated whether they felt high-productivity members should shoulder greater responsibility. Participants also evaluated their own contribution and punishment decisions across all rounds and estimated the corresponding behaviour of the other group members.

Behavioural data acquisition and model-free analysis

To precisely capture real-time interactions and time-stamp every experimental phase, we deployed a web-based platform that enabled four users to participate simultaneously. The application was built with a Vue.js front-end and a MySQL back-end for data capture and storage, recording each participant's contribution and punishment choices every round. WebSocket was employed to synchronize front-ed and back-end communications, enforce a consistent operation sequence across users, and log millisecond-level timestamps for every webpage transition, which were then aligned with the fNIRS neural recordings to achieve precise event marking.

Round-level analysis

We performed a round-level analysis to calculate the mean contributions of high-productivity and low-productivity participants within each round. We additionally calculated (i) the percentage of participants who successfully reached the high, middle, and low thresholds within each round and (ii) the proportion of rounds in which each group reached the threshold (success rate) in NP1, P, and NP2 rounds respectively under coordination. These metrics jointly revealed the distinct behavioural signatures of cooperation and coordination.

Furthermore, we used the wilcoxon rank-sum test to examine the two factors-stage type (NP vs. P) and productivity type (high-productivity vs. low-productivity)-while holding the other factor constant. We paid particular attention to the effect sizes of these tests ($r = Z/\sqrt{N}$), as they quantify inter-sample differences and facilitate direct comparisons. Simultaneously, we examined how the proportion of rounds in which participants successfully reached the threshold under coordination varied between NP and P stage.

Individual-level analysis

First, we modelled the linear relationship between contributions and punishments in the P stage. The predictor was each participant's total contributions. The dependent variables were (i) the total punishments a participant received and (ii) the total punishment a participant imposed (for dimensional consistency, each instance of punishment was scored as the 6 points actually deducted from the

punished). Next, we examined how the paired punishment related to the negative deviation of contributions under both cooperation and coordination, thereby assessing anti-social punishment across different settings [45].

We employed Bayesian linear mixed models (LMMs) to examine individual-level conditional contribution patterns. We modelled each participant's contributions in round t as a function of (i) their own contributions and (ii) the total contributions of other group members in round t-1.

$$C_t^{focal} \sim 1 + C_{t-1}^{focal} + C_{t-1}^{others} + C_{t-1}^{focal} \times C_{t-1}^{others} + (1 + C_{t-1}^{focal} + C_{t-1}^{others} + C_{t-1}^{focal} | individual) \quad (1)$$

Regarding punishment behaviour, we used Bayesian generalized linear mixed models (GLMMs) to model the binary outcome—whether individual i punished individual j in round t—as a function of (i) i's contributions in round t (ii) j's contributions in round t (iii) the amount of punishments i received in round t-1.

$$\begin{aligned} Pun_t^{i \to j} \sim & 1 + C_t^j + C_t^i + C_{t-1}^i + C_t^j \times C_t^i + C_t^i \times C_{t-1}^i + C_{t-1}^i \times C_t^j + C_t^j \times C_t^i \times C_{t-1}^i \\ & + (1 + C_t^j + C_t^i + C_{t-1}^i | individual) \end{aligned} \quad (2)$$

and

$$Pun_t^{i \to j} = \begin{cases} 0 & \text{if i did not punish j} \\ 1 & \text{if i punished j} \end{cases}$$

We estimated stickiness and imitation coefficients separately for behaviour in NP and P stage. Moreover, we examined conditional contribution dynamics, defined as the change in an individual's contributions from the preceding to the current round using the conditional contribution patterns framework. Peer punishment was considered to affect the contribution dynamics of the recipient. In the appendix, we additionally examined the corporate wealth (= contributions × productivity) under cooperation and coordination, and how threshold magnitude and the binary factor whether the threshold was reached (binary: 0 = not reached, 1 = reached) affect both contribution patterns and contribution dynamics under coordination.

Psychological decision-making computational model

To establish a unified computational framework for cooperation and coordination, we fitted 12 distinct models to explain contributions in cooperation and coordination. All models assumed that participants first predicted the others' contributions from their past round behaviour, then computed the expected utility of each possible contributions for themselves, and finally selected the contribution with the category distribution probability. Selecting a higher contribution level reflected participants' willingness to invest more wealth to maximize public resources and benefited the group, whereas opting for a lower contribution level signalled an attempt to preserve personal wealth and minimized investment losses.

We employed two belief updating methods to compute other participants' expected contributions. The first method assumes that participants track the contributions of the other group members via a reinforcement learning rule, dynamically adjusting their own strategies by observing and learning from others' contributions patterns [70]. During this process, participants assigned progressively lower weights to past observations and higher weights to more recent events. This "forgetting the

past" mechanism is particularly well-suited to dynamic environments in which other participants' behavioural patterns may evolve over time. The second method assumes that participants represent their beliefs about others' contributions with a normal prior and update these beliefs via Bayesian inference [67]. Because the experiment only revealed a finite set of discrete contribution levels, using a normal prior allowed the model to capture both the central tendency and dispersion of others' contributions, yielding more accurate posterior estimates in the Bayesian update. Finally, to simplify the model and avoid over-fitting, we assumed that each participant maintained a single set of parameters to update beliefs about all other group members. This is reasonable because the experiment employed anonymous interactions, preventing participant-specific parameterisation.

The components of utility

The self-regarding preference and social preference utility. We adopted the standard framework of game theory and analysed behaviour of each individual, treating one focal participant at one time while holding the remaining three group members as the reference set. In practice, participants were indexed by the integers 1–4, and we denoted the focal player as $focal \in \{1, 2, 3, 4\}$; the complementary set of co-players was then $i \in \{1, 2, 3, 4\} - \{focal\}$. For each focal participant, we modelled an iterated game in which n players interacted across discrete rounds indexed by $t = 1, 2, \ldots$. Each participant began every round with an endowment $e_i = 30$. In round t, every participant i simultaneously selected a contribution $C_{i,t} \in [0, 30]$, yielding the contribution vector $\vec{C}_t = (C_{1,t}, C_{2,t}, C_{3,t}, C_{4,t})$. The payoff vector $\vec{\pi}_t$ was then computed as:

$$\vec{\pi}_t = \begin{cases} \vec{e} - \vec{C}_t + \boldsymbol{P} \cdot \vec{C}_t & \text{coorperation} \\ \vec{e} - \vec{C}_t + \frac{thd_t}{4} \vec{\mathcal{X}}_{\geq thd_t}(\vec{1}' \cdot \boldsymbol{P} \cdot \vec{C}_t) & \text{coordination} \end{cases} \tag{3}$$

where $\boldsymbol{P}$ denotes the productivity matrix, and in this study $\boldsymbol{P} = \frac{1}{4}\vec{\mathbf{1}} \cdot \vec{p}'$, with $\vec{p}$ the productivity vector. Without loss of generality, the focal participant corresponded to the first component of every vector. Given the contribution belief vector $\vec{\mathbb{E}}_t^{focal,c}(C)$ about others' contributions, the utility combining self-regarding and social preferences derived by the focal participant when contributing c is computed as

$$U_t^{focal,c} = \vec{\beta}' \cdot \vec{\pi}_t^{focal,c} = \vec{\beta}' \cdot \left(\vec{e} - \vec{\mathbb{E}}_t^{focal,c}(C) + \boldsymbol{P} \cdot \vec{\mathbb{E}}_t^{focal,c}(C)\right) \tag{4}$$

where

$$\vec{\beta} = \begin{bmatrix} 1 \\ \beta^{focal} \\ \beta^{focal} \\ \beta^{focal} \end{bmatrix}$$

$$\vec{\mathbb{E}}_t^{focal,c}(C) = \begin{bmatrix} c \\ \mathbb{E}_{i,t}^{focal}(C) \end{bmatrix} = \begin{bmatrix} c \\ \mathbb{E}_{i_1,t}^{focal}(C) \\ \mathbb{E}_{i_2,t}^{focal}(C) \\ \mathbb{E}_{i_3,t}^{focal}(C) \end{bmatrix}$$

β_{focal} denotes the social preferences parameter, defined as the relative weight of social preferences to self-regarding preferences (with the latter normalized to 1). The indices $i_1, i_2, i_3 \in \{1, 2, 3, 4\} \setminus \{\text{focal}\}$ enumerate the other group members. We allowed β_{focal} to vary linearly with the expected contributions of other group members as follows:

$$\beta_{focal} = \beta_{slope}(\mathbb{E}^{focal}_{i_1,t}(C) + \mathbb{E}^{focal}_{i_2,t}(C) + \mathbb{E}^{focal}_{i_3,t}(C)) + \beta_{intercept} \tag{5}$$

The social norms utility. Experimental contribution behaviour was inconsistent with the pure rational model: their observed action could not be explained if all participants were fully rational and selfish. When free-riding was the dominant strategy in both cooperation and coordination, especially cooperation, agents would neither contribute nor sacrifice cost to punish in order to promote contributing. Nevertheless, social norms which are conceptualized as widespread expectations that others approve or disapprove of a behaviour, sanction it, and view such sanctions as legitimate, resolve this dilemma [15]. Here, we defined the focal participant's social norms utility as the "prejudice" that the participant imposed on his own alternative contributions after accounting for the influence of the other group members [41]. This constituted a second-order norm: participants were motivated to infer how others evaluated specific contribution and to internalised the responsibilities they were expected to assume within the group [4]. Intuitively, social norms generate non-zero, typically negative—utility, for low contribution options, thereby shifting the probability of selecting those options. Formally, this is defined as:

$$U^{focal,c}_T = \begin{cases} -\gamma(c - c^*_T)^2 & \text{if } c < c^*, \\ 0 & \text{if } c \geq c^*, \end{cases} \tag{6}$$

Here, c^*_t denotes the minimal contribution level consistent with the normative provisions and captures the overall contribution level of the group. Following Gavrilets et al [58], we specified it as mean contributions of past rounds:

$$c^*_T = \frac{\sum_{t=T-t_0}^{T-1} \sum_{i=1}^{4} C_{i,t}}{4t_0} \tag{7}$$

Here, we set the rounds $t_0 = 2$ for participants' retrospective historical memory. On one hand, one-step memory is incapable of forming a stable social consensus. On the other hand, given that people's limited memory in reality cannot remember decisions made more than two rounds ago, we referred to the setting in previous research [41, 58] and found it produced a good enough fitting effect on real behaviour.

Tracking of other participants' contribution beliefs

Reinforcement learning. At its core, reinforcement learning enables agents to learn from past actions and to update their expectations about future events by progressively down-weighting older observations and up-weighting the most recent ones. The update rule allows participants to adapt rapidly to shifting environmental conditions while diminishing the impact of early mis-estimates. We implemented a Rescorla–Wagner reinforcement learning rule. The model assumed that the focal participant updated the expected contributions $mathbbefocal_i(t)$ of the participant i according to the prediction error δ. Specifically, the prediction error $\delta = C_{i,t-1} - \mathbb{E}^{focal}_{i,t-1}(C)$ reflected the difference between the predicted contributions and the actual contributions of the participant i in the $t-1$ round. According to Rescorla-Wagner rule, the updated formula of expected contributions is:

$$\mathbb{E}^{focal}_{i,t}(C) = \mathbb{E}^{focal}_{i,t-1}(C) + \alpha^{focal}\delta = \mathbb{E}^{focal}_{i,t-1}(C) + \alpha^{focal}(C_{i,t-1} - \mathbb{E}^{focal}_{i,t-1}(C)) \tag{8}$$

Here, α^{focal} denotes the focal participant's learning rate: the higher α^{focal}, the more rapidly the focal participant revises his beliefs about others' contributions, giving greater weight to their most

recent actions. Formally, this reinforcement-learning update is equivalent to Bayesian inference under a Dirichlet prior.

Bayesian updating with the normal distribution. This method iteratively updates the focal participant's belief about participant i's contributions from a Gaussian prior $\mathcal{N}(\mu_{i,0}, \sigma_{i,0})$, Upon observing the real contribution $C_{i,t-1}$, the posterior belief becomes $\mathbb{E}_{i,t}^{focal}(C) \sim \mathcal{N}(\mu_{i,t}, \sigma_{i,t})$, implying the generative model $C_{i,t} \sim \mathcal{N}(\mathbb{E}_{i,t}^{focal}(C), \sigma_{focal}^2)$, The update rules are as follows:

$$\begin{aligned} \mu_{i,t} &= \frac{\sigma_{i,t-1}^2 C_{i,t-1} + \sigma_{focal}^2 \mu_{i,t-1}}{\sigma_{i,t-1}^2 + \sigma_{focal}^2} \\ \sigma_{i,t}^2 &= \frac{\sigma_{i,t-1}^2 \sigma_{focal}^2}{\sigma_{i,t-1}^2 + \sigma_{focal}^2} \end{aligned} \tag{9}$$

where σ_{focal}^2 represents the learning observation variance of the model.

The utility-based models

Variable-weight SON model, v-SON. We assumed that participants integrated self-regarding preferences, social preferences, and social norms when selecting their contribution in each round leveraging the aforementioned utility components (i.e., $\beta_{focal} \not\equiv 0, \gamma \not\equiv 0$). Under the variable-weight specification, the social preferences parameter is allowed to vary dynamically with the expected contributions of others (i.e., $\beta_{slope} \not\equiv 0$).

Fixed-weight SON model, f-SON. When participants remain largely insensitive to others' contributions throughout the experiment, the social preferences parameter stays constant and is unaffected by others' behaviour (i.e., $\beta_{slope} \equiv 0$), and all three utility components are retained (i.e., $\beta_{focal} \not\equiv 0, \gamma \not\equiv 0$).

Variable-weight SO model, v-SO. Building on the v-SON model, if participants disregard the additional utility supplied by social norms, the resulting specification becomes the v-SO model (i.e., $\beta_{focal} \equiv 0, \gamma \not\equiv 0, \beta_{slope} \not\equiv 0$).

Fixed-weight SO model, f-SO. Building on the f-SON model, if participants disregard the additional utility supplied by social norms, the resulting specification becomes the f-SO model (i.e., $\beta_{focal} \equiv 0, \gamma \not\equiv 0, \beta_{slope} \equiv 0$).

Independent social norms model, N. We specified a model in which participants disregard the welfare of others; accordingly, only social norms utility is retained (i.e., $\beta_{focal} \equiv 0, \gamma \not\equiv 0$).

Finally, following traditional game theoretic method of deriving contribution rates from payoffs, we defined the baseline model as one in which participants consider only their own monetary payoff in the next round (i.e., $\beta_{focal} \equiv 0, \gamma \equiv 0$). For cooperation and coordination, we derived 12 distinct models by crossing the six utility component specifications with two belief updating rules (reinforcement learning vs. Bayesian updating with a normal prior), yielding 12 models for cooperation and coordination.

Model fitting and model selection

We separately estimated the parameters of utility-based models for NP1, P, and NP2 rounds of each participant, assuming that a single parameter set governed behaviour within each round type. Maximum-likelihood estimates were obtained via grid search over uniformly distributed parameter grids. Specifically, we fitted the model parameters for each participant by maximizing the summed log-likelihood of the observed contributions. For any specific contribution c, the selection probability was computed via the softmax function applied to the combined utility:

$$P(c) = \frac{\exp(U(c)^T)}{\exp(\sum_c U(c)^T)}$$

Here, T denotes the inverse-temperature parameter. Initial historical contribution and group members' contribution beliefs were seeded with the two rounds preceding each fitting window (for NP1, these came from the practice rounds). Separate memory spaces were maintained for each threshold level under coordination to store the corresponding historical contributions and beliefs.

We computed the Bayesian Information Criterion (BIC) for each participant within each round type using the maximised log-likelihood LL. Specifically, BIC was calculated as

$$\text{BIC} = -2\,LL + m\,\ln R,$$

where m denotes the number of estimated parameters and R the number of rounds.

We calibrated the minimum BIC across all candidate models for every participant within each round type, treating each participant in a certain round (NP1, P, NP2) as an independent observation. Using these BIC values, we then implemented a random-effects Bayesian Model Selection (BMS) routine, yielding exceedance probabilities and expected posterior model frequencies. On this basis, we identified the winning models for the cooperation and coordination, respectively.

Model evolution process

We examined how the SON model parameters collectively affect the contribution ratio in cooperation and coordination. Using the winning models for cooperation and coordination, we conducted out-of-sample simulations (i.e., without real behavioural data) to test how combinations of rational (self-regarding and social preferences) and social norms parameters jointly determine the equilibrium contribution ratio. In particular, the simulations replicate the experimental four-person PGGs. We initialised four agents with identical parameter values and permitted their selections to evolve according to the winning model. Specifically, under cooperation, we investigated how the interactions between γ and α, γ and β_{slope}, and γ and $\beta_{intercept}$ affect the final contribution ratio. Under coordination, we investigated how the interactions between γ and α, γ and $\beta_{intercept}$ affect the final contribution ratio. For parameters excluded from the investigation in each simulation, we fixed their values at the respective means obtained from the fitted models. All evolutionary simulations began with a 2×4 contribution matrix randomly drawn from the experimental range, and initial beliefs about others' contributions were set to the mean of these two historical rounds. Building on this setup, we simulated 100 rounds per parameter set, as contributions reached steady state within this horizon. Each parameter combination was simulated 100 times, and the resulting contributions were averaged across runs to yield the final simulation outcome for that set.

fNIRS data acquisition

Neural data from all four participants was acquired simultaneously with the ETG-4100 optical topography system (Hitachi Medical Corporation). The system samples at 10 Hz and employed near-infrared wavelengths of 695 nm and 830 nm. We used four identical customized optode probe sets, each with two sets of probes. Optode positions were localised according to the international 10–10 system using the fNIRS Optodes' Location Decider [93]. The first probe set was positioned over the dorsal medial prefrontal cortex, with its posterior optode centred at Fz (Supplementary Figure). The second probe set covered the right temporoparietal junction, aligned so that its upper-left photodiode was placed at CP6 (Supplementary Figure). Each probe set comprised four measurement channels—two emitters and two detectors spaced 30 mm apart. Channels 1–4 sampled the medial

prefrontal cortex, whereas channels 5–8 targeted the right temporoparietal junction [94]. Before every session, all optode arrays were inspected and repositioned as needed to ensure consistent placement both within and across participant groups. Following the modified Beer–Lambert law, concentration changes in HbO and HbR were extracted from each channel. Because HbO is the most sensitive haemodynamic variable and shows a strong positive correlation with the BOLD signal, only HbO concentration changes were analysed.

fNIRS data processing

Data preprocessing

The cooperative and coordinative environments may elicit distinct patterns of within- and between-individual neural responses during social interaction [46]. We focus on three levels of neural response: (1) intra-individual activation patterns; (2) functional connectivity patterns between the dmPFC and the rTPJ within each participant; and (3) inter-individual neural synchronization patterns, quantified by the mean group-level synchronisation index. The raw fNIRS data were first detrended using a DCT high-pass filter with a 128-s cut-off, and temporal autocorrelation was corrected via a pre-colouring approach whose filter shape is hrf transfer function [95].

Based on the investment and punishment phases used in the experiment, we defined the time windows for intra-individual activation analysis. Given the timing differences between NP and P stage, we defined the selection phase (5 s thinking about round contribution + 7 s seleting round contribution; see Supplementary Information) as the operation phase, during which participants thought and made behavioural selections. This was taken to mark the cycle time of the neural patterns in this study.

Intra-individual neural activation patterns

Because the first 10 s of each operation phase was occupied by waiting or outcome feedback, we defined the first 10 s of each operation phase as the baseline phase (see Figure 4). Brain activation patterns were calculated as the increase in HbO concentration during the operation phase relative to the baseline phase. Specifically, we performed z-scoring on the operation phase data using the mean and standard deviation of the baseline phase data. For the two regions of interest, we first calculated the mean activation for each individual across NP1, P, and NP2 rounds under cooperation and coordination respectively to check for differences in brain activation patterns between the two mechanisms. These individual-level data were then averaged across all participants within each round to yield trial level data (see Figure **??**). Second, we calculated the mean activation patterns across all three round types for each individual and regressed these against the mean contributions/punishments imposed by each participant to examine the relationship between brain activation and overall contributions under cooperation and coordination.

Neural functional connectivity patterns

To explore the similarities and differences in functional connectivity between individual brain regions under cooperation and coordination, we used wavelet coherence (WTC) to calculate the coherence values between different channels of the dmPFC and rTPJ, thereby defining the functional connectivity patterns of the dmPFC–rTPJ link. First, we calculated the coherence values for each paired channel (each of the four channels in dmPFC with each of the four channels in rTPJ, yielding 16 channel pairs) and transformed these values via Fisher z-transformation to obtain the functional connectivity.

Similar to the activation patterns, we calculated the mean functional connectivity across all three round types for each individual and regressed these against the mean contributions or punishments imposed by each participant to examine the relationship between functional connectivity and overall contributions under cooperation and coordination.

Inter-individual neural synchronization patterns

We used wavelet coherence analysis to calculate the cross-correlation between preprocessed neural time series among participants as a function of frequency and time. The coherence value during the pre-experiment resting state was defined as the baseline, and the increase in coherence during the operation phase relative to this resting-state coherence (after Fisher z-transformation) was defined as the inter-individual neural synchronization (INS) patterns in this study. First, we identified the frequency bands of interest by calculating the mean wavelet coherence between all participant pairs in the experiments, averaging across 142 frequency bands and 8 channels, and extracting the difference between the mean coherence value during the experiment and that during the resting state. Compared with the resting state, the frequency band from 0.1219 Hz to 0.1536 Hz (corresponding to the period between 6.5 s and 8.5 s) showed a significant increase in the mean coherence value of the operation phase, and it can be compared with the time period selected by the behaviour (see Figure **??**). This frequency band also excludes high-frequency noise caused by head movement and low-frequency noise related to breathing (about 0.2 to 0.3 Hz) and heart beat (about 1 Hz). Based on this, we focused on analysing the data in this frequency band.

Next, we identified the channels with significant differences. We first averaged the INS of the frequency of interest (FOI) determined in the first step across participants (i.e., averaged the INS of each individual in the investment phase of a specific round). We then averaged the six pairs of INS patterns formed within each group (Figure 6a) and tested whether the resulting mean INS patterns were significantly greater than zero. Building on this, to explore whether there are differences in the INS patterns of cooperation and coordination in some brain regions, we compared whether there are differences in the INS patterns of each channel in all round types under cooperation and coordination.

To verify that the INS patterns were specific to real interacting pairs, a pseudo-group nonparametric permutation test is necessary. We generated pseudo-groups while maintaining the original mechanism (cooperation or coordination). We repeatedly created 1000 different pseudo-groups in each condition and calculated INS patterns based on these pseudo-groups, following the same procedure as for real groups. To ensure that real interacting pairs did not persist in the pseudo-groups, we deliberately assigned participants from the same group to different pseudo-groups, ensuring that no pseudo-group included participants from the same real group (Figure 6c). We applied a nonparametric permutation test based on the pseudo-group INS patterns. For different channels, we calculated the statistics for all pseudo-group INS patterns via one-sample test (against 0). Then, we utilized the independent samples t-test to assess the statistical differences between pseudo-groups in cooperation and coordination. Finally, we compared the statistics of the real group t_0 with the statistics of the pseudo-groups $T_1, T_2, \ldots, T_B$ (where B is the number of permutations). The corresponding permutation test p-value was calculated as:

$$p \approx \frac{1}{B} \sum_{j=1}^{B} I(t_j > t_0)$$

where I is the indicator function.

To explore the relationship between INS and behavioural interactions, we first quantified the correlation between participants' behaviour. As cosine similarity method is more suitable for

sparse nonlinear data, we calculated the cosine similarity of the participants' contribution vectors **Contribution behaviour similarity** $= \frac{\vec{Ctr}_A \cdot \vec{Ctr}_B}{\|\vec{Ctr}_A\|\|\vec{Ctr}_B\|}$ and the sum of wealth spent on punishing each other in P stage **Mutual punishments** $= \sum_{r=22}^{36} (Pun_r^{A\to B} + Pun_r^{B\to A})$. We used each participant pair as a unit to linearly regress the behaviour correlation with the INS of the corresponding operation phase.

Analysis plan

All analyses and final result visualizations were completed using R version 4.3.1 and MATLAB R2022a.

For the behavioural data, we used the R package BRMS version 2.22.0 [96] to fit a Bayesian mixed recursive model for analysing conditional behaviour patterns. For the conditional punishment patterns, we applied a generalized linear mixed model with a Bernoulli distribution as the prior. The remaining fits used ordinary linear mixed models with the default priors of the brms package, as the ample data rendered the priors unlikely to influence coefficient estimation. During fitting, independent variables were standardized to have a mean of 0 and a standard deviation of 1, except for paired punishment variables, which were binary nominal variables. Other dependent variables were also standardized to have a mean of 0 and a standard deviation of 1. To account for repeated measurements, all regression models included random intercepts for participants and random slopes for the independent variables corresponding to each model. In addition to report the posterior means of the β values and correlation values, we also provided the highest density intervals (HDI) calculated using the bayestestR package (version 0.15.2). When employing the Markov chain Monte Carlo (MCMC) method, the number of warm-up iterations was set to 1000, the number of post-warm-up iterations to 3000, and the number of chains to 10. In all analyses, the $\hat{R}$ statistics were below 1.05, indicating convergence of the MCMC method. The Bulk-ESS and Tail-ESS values for all model parameters were high, indicating high accuracy of the models. For the parameter fitting of the psychological decision-making computational model, we used the 'fmincon' function in MATLAB to find the parameters that minimize the negative log-likelihood value. To increase the probability of finding the global minimum, we repeated the search process 500 times with different starting points. We then used the Bayesian Information Criterion (BIC) of each participant in each model across three round types to implement the random-effects Bayesian Model Selection (BMS) routine via the VBA toolbox [97]) derived from MATLAB.

For the neural data, the raw neural data was preprocessed using MATLAB functions based on the NIRS-SPM package [95], and wavelet coherence between pairs of neural time series was calculated using the built-in WTC function in MATLAB. Differences in neural data between cooperation and coordination were compared, with FDR-corrected p-values applied in the corresponding brain regions.

Acknowledgements

This work is supported by National Science and Technology Major Project (2022ZD0116800), Program of National Natural Science Foundation of China (12425114, 62141605, 12201026,12301305), the Fundamental Research Funds for the Central Universities, Beijing Natural Science Foundation(Z230001), and the China Postdoctoral Science Foundation (2025M774219).

Author contributions

Y.L. and X.W. conceived the project and designed the experiments. Y.L., X.W., W.D., L.L., Y.Y., Y.Z. and Y.Z. organized the experiments and collected the data. Y.L., X.W., W.D. and L.L. analysed

the data and prepared the figures. Y.L. and X.W. developed the computational model and interpreted the results. Y.L., X.W. and S.T. wrote the original and final version of the manuscript. X.W., S.T. and H.Z. funded and supervised the project.

Competing interests

The authors declare no competing interests.

Correspondence and requests for materials should be addressed to Xin Wang or Shaoting Tang.

References

[1] Skyrms, B. *Evolution of the social contract* (Cambridge University Press, 2014).

[2] Santos, L. R. & Rosati, A. G. The evolutionary roots of human decision making. *Annual review of psychology* **66**, 321–347 (2015).

[3] Buyalskaya, A., Gallo, M. & Camerer, C. F. The golden age of social science. *Proceedings of the National Academy of Sciences* **118**, e2002923118 (2021).

[4] El Zein, M., Bahrami, B. & Hertwig, R. Shared responsibility in collective decisions. *Nature human behaviour* **3**, 554–559 (2019).

[5] Van Lange, P. A., Joireman, J., Parks, C. D. & Van Dijk, E. The psychology of social dilemmas: A review. *Organizational Behavior and Human Decision Processes* **120**, 125–141 (2013).

[6] Hardin, G. The tragedy of the commons: the population problem has no technical solution; it requires a fundamental extension in morality. *science* **162**, 1243–1248 (1968).

[7] Fundenberg, D. & Maskin, E. Evolution and cooperation in noisy repeated games. *The American Economic Review* **80**, 274–279 (1990).

[8] Schmid, L., Chatterjee, K., Hilbe, C. & Nowak, M. A. A unified framework of direct and indirect reciprocity. *Nature Human Behaviour* **5**, 1292–1302 (2021).

[9] FeldmanHall, O. & Nassar, M. R. The computational challenge of social learning. *Trends in Cognitive Sciences* **25**, 1045–1057 (2021).

[10] Khalvati, K. *et al.* Modeling other minds: Bayesian inference explains human choices in group decision-making. *Science advances* **5**, eaax8783 (2019).

[11] Jordan, J. J. A pull versus push framework for reputation. *Trends in Cognitive Sciences* **27**, 852–866 (2023).

[12] Akata, E. *et al.* Playing repeated games with large language models. *Nature Human Behaviour* 1–11 (2025).

[13] Elster, J. & Jon, E. The cement of society: A study of social order (1989).

[14] Zhang, W. *Game theory and society* (Routledge, 2017).

[15] Horne, C. & Mollborn, S. Norms: An integrated framework. *Annual Review of Sociology* **46**, 467–487 (2020).

[16] Fischbacher, U. & Gächter, S. Social preferences, beliefs, and the dynamics of free riding in public goods experiments. *American economic review* **100**, 541–556 (2010).

[17] Wilson, R. K. The contribution of behavioral economics to political science. *Annual Review of Political Science* **14**, 201–223 (2011).

[18] Hilbe, C., Wu, B., Traulsen, A. & Nowak, M. A. Cooperation and control in multiplayer social dilemmas. *Proceedings of the National Academy of Sciences* **111**, 16425–16430 (2014).

[19] Brian, D. *Pulitzer: a life* (John Wiley & Sons, 2002).

[20] Von Neumann, J. & Morgenstern, O. in *Theory of games and economic behavior: 60th anniversary commemorative edition* (Princeton university press, 2007).

[21] Hauser, O. P., Hilbe, C., Chatterjee, K. & Nowak, M. A. Social dilemmas among unequals. *Nature* **572**, 524–527 (2019).

[22] Hübner, V., Staab, M., Hilbe, C., Chatterjee, K. & Kleshnina, M. Efficiency and resilience of cooperation in asymmetric social dilemmas. *Proceedings of the National Academy of Sciences* **121**, e2315558121 (2024).

[23] Wang, X. *et al.* Cooperation and coordination in heterogeneous populations. *Philosophical Transactions of the Royal Society B* **378**, 20210504 (2023).

[24] Mori, R., Hanaki, N. & Kameda, T. An outside individual option increases optimism and facilitates collaboration when groups form flexibly. *Nature Communications* **15**, 5520 (2024).

[25] Rand, D. G. & Nowak, M. A. The evolution of antisocial punishment in optional public goods games. *Nature communications* **2**, 434 (2011).

[26] Lee, D. Game theory and neural basis of social decision making. *Nature neuroscience* **11**, 404–409 (2008).

[27] Rilling, J. K. *et al.* A neural basis for social cooperation. *Neuron* **35**, 395–405 (2002).

[28] Park, S. A., Sestito, M., Boorman, E. D. & Dreher, J.-C. Neural computations underlying strategic social decision-making in groups. *Nature communications* **10**, 5287 (2019).

[29] Konovalov, A., Hill, C., Daunizeau, J. & Ruff, C. C. Dissecting functional contributions of the social brain to strategic behavior. *Neuron* **109**, 3323–3337 (2021).

[30] Hill, C. A. *et al.* A causal account of the brain network computations underlying strategic social behavior. *Nature neuroscience* **20**, 1142–1149 (2017).

[31] Suzuki, S. *et al.* Learning to simulate others' decisions. *Neuron* **74**, 1125–1137 (2012).

[32] Pisauro, M. A., Fouragnan, E., Arabadzhiyska, D., Apps, M. A. & Philiastides, M. G. Neural implementation of computational mechanisms underlying the continuous trade-off between cooperation and competition. *Nature Communications* **13**, 6873 (2022).

[33] Philippe, R. *et al.* Neurocomputational mechanisms involved in adaptation to fluctuating intentions of others. *Nature communications* **15**, 3189 (2024).

[34] Jiang, Y., Mi, Q. & Zhu, L. Neurocomputational mechanism of real-time distributed learning on social networks. *Nature neuroscience* **26**, 506–516 (2023).

[35] Buckholtz, J. W. & Marois, R. The roots of modern justice: cognitive and neural foundations of social norms and their enforcement. *Nature neuroscience* **15**, 655–661 (2012).

[36] Suzuki, S., Adachi, R., Dunne, S., Bossaerts, P. & O'Doherty, J. P. Neural mechanisms underlying human consensus decision-making. *Neuron* **86**, 591–602 (2015).

[37] Feng, C., Tian, X. & Luo, Y.-J. Neurocomputational substrates underlying the effect of identifiability on third-party punishment. *Journal of Neuroscience* **43**, 8018–8031 (2023).

[38] Banerjee, A. V. A simple model of herd behavior. *The quarterly journal of economics* **107**, 797–817 (1992).

[39] Molinaro, G. & Collins, A. G. A goal-centric outlook on learning. *Trends in Cognitive Sciences* **27**, 1150–1164 (2023).

[40] De Martino, B. & Cortese, A. Goals, usefulness and abstraction in value-based choice. *Trends in Cognitive Sciences* **27**, 65–80 (2023).

[41] Fehr, E. & Schurtenberger, I. Normative foundations of human cooperation. *Nature human behaviour* **2**, 458–468 (2018).

[42] Van Dijk, E. & De Dreu, C. K. Experimental games and social decision making. *Annual Review of Psychology* **72**, 415–438 (2021).

[43] Falk, A. & Heckman, J. J. Lab experiments are a major source of knowledge in the social sciences. *science* **326**, 535–538 (2009).

[44] Gachter, S., Renner, E. & Sefton, M. The long-run benefits of punishment. *Science* **322**, 1510–1510 (2008).

[45] Fehr, E. & Gächter, S. Altruistic punishment in humans. *Nature* **415**, 137–140 (2002).

[46] Kingsbury, L. & Hong, W. A multi-brain framework for social interaction. *Trends in neurosciences* **43**, 651–666 (2020).

[47] Lockwood, P. L., Apps, M. A. & Chang, S. W. Is there a 'social'brain? implementations and algorithms. *Trends in cognitive sciences* **24**, 802–813 (2020).

[48] Xie, H. *et al.* Finding the neural correlates of collaboration using a three-person fmri hyper-scanning paradigm. *Proceedings of the National Academy of Sciences* **117**, 23066–23072 (2020).

[49] Pinti, P. *et al.* The present and future use of functional near-infrared spectroscopy (fnirs) for cognitive neuroscience. *Annals of the new York Academy of Sciences* **1464**, 5–29 (2020).

[50] Stangl, M., Maoz, S. L. & Suthana, N. Mobile cognition: imaging the human brain in the 'real world'. *Nature Reviews Neuroscience* **24**, 347–362 (2023).

[51] Ruff, C. C. & Fehr, E. The neurobiology of rewards and values in social decision making. *Nature Reviews Neuroscience* **15**, 549–562 (2014).

[52] Padilla-Coreano, N., Tye, K. M. & Zelikowsky, M. Dynamic influences on the neural encoding of social valence. *Nature Reviews Neuroscience* **23**, 535–550 (2022).

[53] Wu, Y. E. & Hong, W. Neural basis of prosocial behavior. *Trends in Neurosciences* **45**, 749–762 (2022).

[54] Bilek, E. *et al.* Information flow between interacting human brains: Identification, validation, and relationship to social expertise. *Proceedings of the National Academy of Sciences* **112**, 5207–5212 (2015).

[55] Loewenstein, G. & Molnar, A. The renaissance of belief-based utility in economics. *Nature Human Behaviour* **2**, 166–167 (2018).

[56] Tump, A. N., Deffner, D., Pleskac, T. J., Romanczuk, P. & M. Kurvers, R. H. A cognitive computational approach to social and collective decision-making. *Perspectives on Psychological Science* **19**, 538–551 (2024).

[57] Gächter, S., Molleman, L. & Nosenzo, D. Why people follow rules. *Nature Human Behaviour* 1–13 (2025).

[58] Gavrilets, S., Tverskoi, D. & Sánchez, A. Modelling social norms: an integration of the norm-utility approach with beliefs dynamics. *Philosophical Transactions of the Royal Society B* **379**, 20230027 (2024).

[59] Kölle, F. Heterogeneity and cooperation: The role of capability and valuation on public goods provision. *Journal of Economic Behavior & Organization* **109**, 120–134 (2015).

[60] Noussair, C. N. & Tan, F. Voting on punishment systems within a heterogeneous group. *Journal of Public Economic Theory* **13**, 661–693 (2011).

[61] Herrmann, B., Thoni, C. & Gachter, S. Antisocial punishment across societies. *Science* **319**, 1362–1367 (2008).

[62] Press, W. H. & Dyson, F. J. Iterated prisoner's dilemma contains strategies that dominate any evolutionary opponent. *Proceedings of the National Academy of Sciences* **109**, 10409–10413 (2012).

[63] Van Veelen, M., García, J., Rand, D. G. & Nowak, M. A. Direct reciprocity in structured populations. *Proceedings of the National Academy of Sciences* **109**, 9929–9934 (2012).

[64] Lee, J. K., Rouault, M. & Wyart, V. Adaptive tuning of human learning and choice variability to unexpected uncertainty. *Science Advances* **9**, eadd0501 (2023).

[65] Dong, Y., Zhang, B. & Tao, Y. The dynamics of human behavior in the public goods game with institutional incentives. *Scientific Reports* **6**, 28809 (2016).

[66] Toyokawa, W., Whalen, A. & Laland, K. N. Social learning strategies regulate the wisdom and madness of interactive crowds. *Nature Human Behaviour* **3**, 183–193 (2019).

[67] Khalvati, K., Kiani, R. & Rao, R. P. Bayesian inference with incomplete knowledge explains perceptual confidence and its deviations from accuracy. *Nature communications* **12**, 5704 (2021).

[68] Burton-Chellew, M. N. & West, S. A. Payoff-based learning best explains the rate of decline in cooperation across 237 public-goods games. *Nature human behaviour* **5**, 1330–1338 (2021).

[69] Brock, W. A. & Durlauf, S. N. Discrete choice with social interactions. *The Review of Economic Studies* **68**, 235–260 (2001).

[70] Ting, C.-C., Salem-Garcia, N., Palminteri, S., Engelmann, J. B. & Lebreton, M. Neural and computational underpinnings of biased confidence in human reinforcement learning. *Nature Communications* **14**, 6896 (2023).

[71] Redcay, E. & Schilbach, L. Using second-person neuroscience to elucidate the mechanisms of social interaction. *Nature Reviews Neuroscience* **20**, 495–505 (2019).

[72] Molleman, L., Kölle, F., Starmer, C. & Gächter, S. People prefer coordinated punishment in cooperative interactions. *Nature Human Behaviour* **3**, 1145–1153 (2019).

[73] Rand, D. G., Greene, J. D. & Nowak, M. A. Spontaneous giving and calculated greed. *Nature* **489**, 427–430 (2012).

[74] Zoh, Y., Chang, S. W. & Crockett, M. J. The prefrontal cortex and (uniquely) human cooperation: a comparative perspective. *Neuropsychopharmacology* **47**, 119–133 (2022).

[75] Yang, J., Zhang, H., Ni, J., De Dreu, C. K. & Ma, Y. Within-group synchronization in the prefrontal cortex associates with intergroup conflict. *Nature neuroscience* **23**, 754–760 (2020).

[76] Makovi, K., Sargsyan, A., Li, W., Bonnefon, J.-F. & Rahwan, T. Trust within human-machine collectives depends on the perceived consensus about cooperative norms. *Nature communications* **14**, 3108 (2023).

[77] Aumann, R. J. A synthesis of behavioural and mainstream economics. *Nature human behaviour* **3**, 666–670 (2019).

[78] Rand, D. G. & Nowak, M. A. Human cooperation. *Trends in cognitive sciences* **17**, 413–425 (2013).

[79] Aguinis, H., Rupp, D. E. & Glavas, A. Corporate social responsibility and individual behaviour. *Nature Human Behaviour* **8**, 219–227 (2024).

[80] Rasanan, A. H. H. *et al.* Beyond discrete-choice options. *Trends in Cognitive Sciences* (2024).

[81] McAvoy, A. & Hauert, C. Autocratic strategies for iterated games with arbitrary action spaces. *Proceedings of the National Academy of Sciences* **113**, 3573–3578 (2016).

[82] Alvarez-Rodriguez, U. *et al.* Evolutionary dynamics of higher-order interactions in social networks. *Nature Human Behaviour* **5**, 586–595 (2021).

[83] Ferraz de Arruda, G., Aleta, A. & Moreno, Y. Contagion dynamics on higher-order networks. *Nature Reviews Physics* **6**, 468–482 (2024).

[84] Han, Z. *et al.* Probabilistic activity driven model of temporal simplicial networks and its application on higher-order dynamics. *Chaos: An Interdisciplinary Journal of Nonlinear Science* **34** (2024).

[85] Liu, L., Zheng, H., Han, Z., Wang, X. & Tang, S. Higher-order network adaptivity: co-evolution of higher-order structure and spreading dynamics. *arXiv preprint arXiv:2508.15445* (2025).

[86] Tsvetkova, M., Yasseri, T., Pescetelli, N. & Werner, T. A new sociology of humans and machines. *Nature Human Behaviour* **8**, 1864–1876 (2024).

[87] Allen, K. *et al.* Using games to understand the mind. *Nature human behaviour* **8**, 1035–1043 (2024).

[88] Faul, F., Erdfelder, E., Buchner, A. & Lang, A.-G. Statistical power analyses using g* power 3.1: Tests for correlation and regression analyses. *Behavior research methods* **41**, 1149–1160 (2009).

[89] Falk, A., Becker, A., Dohmen, T., Huffman, D. & Sunde, U. The preference survey module: A validated instrument for measuring risk, time, and social preferences. *Management Science* **69**, 1935–1950 (2023).

[90] Murphy, R. O., Ackermann, K. A. & Handgraaf, M. J. Measuring social value orientation. *Judgment and Decision making* **6**, 771–781 (2011).

[91] Houser, D. & Kurzban, R. Revisiting kindness and confusion in public goods experiments. *American Economic Review* **92**, 1062–1069 (2002).

[92] Wang, G., Li, J., Wang, W., Niu, X. & Wang, Y. Confusion cannot explain cooperative behavior in public goods games. *Proceedings of the National Academy of Sciences* **121**, e2310109121 (2024).

[93] Zimeo Morais, G. A., Balardin, J. B. & Sato, J. R. fnirs optodes' location decider (fold): a toolbox for probe arrangement guided by brain regions-of-interest. *Scientific reports* **8**, 3341 (2018).

[94] Liu, T., Duan, L., Dai, R., Pelowski, M. & Zhu, C. Team-work, team-brain: exploring synchrony and team interdependence in a nine-person drumming task via multiparticipant hyperscanning and inter-brain network topology with fnirs. *NeuroImage* **237**, 118147 (2021).

[95] Ye, J. C., Tak, S., Jang, K. E., Jung, J. & Jang, J. Nirs-spm: statistical parametric mapping for near-infrared spectroscopy. *Neuroimage* **44**, 428–447 (2009).

[96] Bürkner, P.-C. brms: An r package for bayesian multilevel models using stan. *Journal of statistical software* **80**, 1–28 (2017).

[97] Daunizeau, J., Adam, V. & Rigoux, L. Vba: a probabilistic treatment of nonlinear models for neurobiological and behavioural data. *PLoS computational biology* **10**, e1003441 (2014).